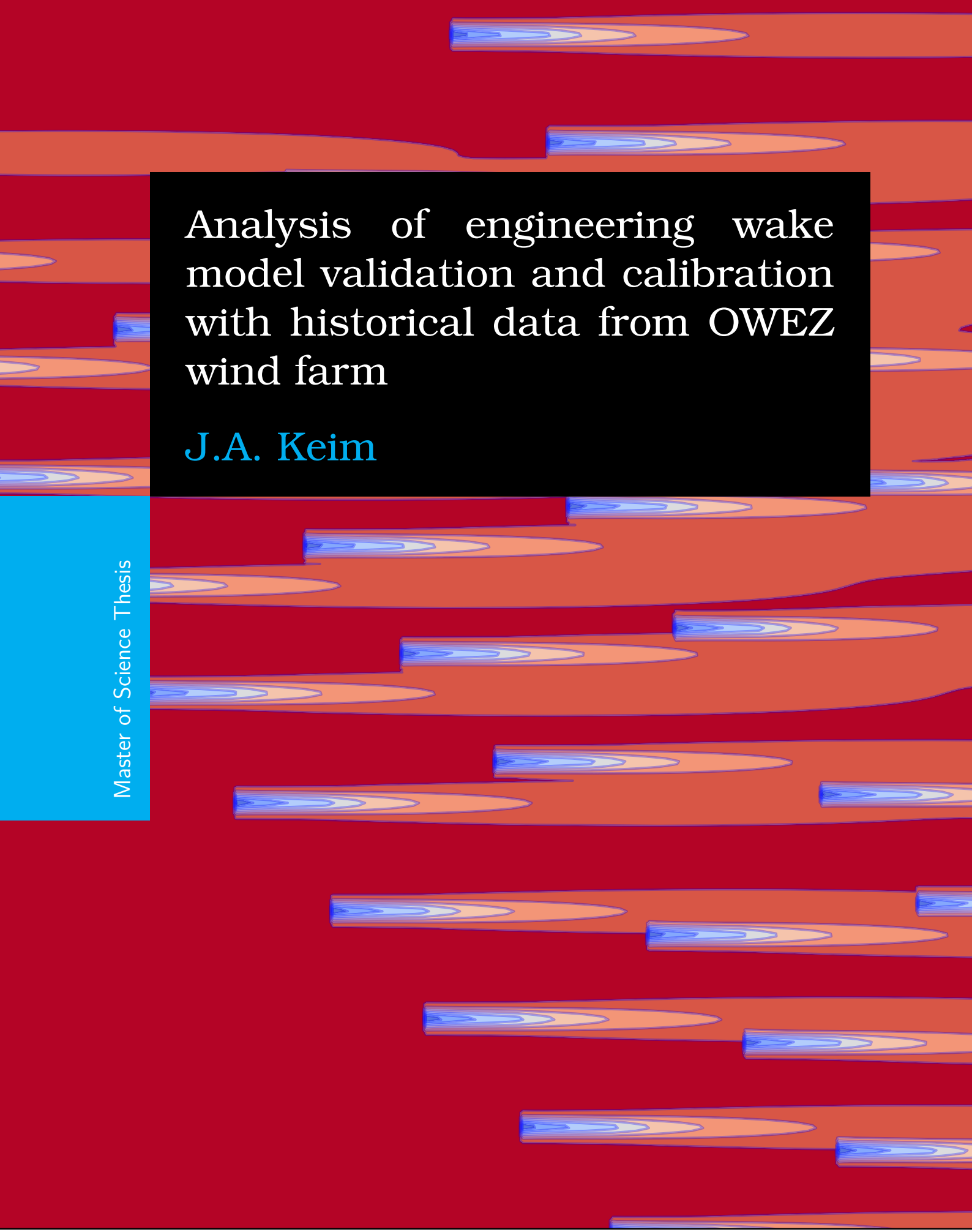

Analysis of engineering wake model validation and calibration with historical data from OWEZ wind farm

J.A. Keim

Master of Science Thesis

TU Delft Delft University of Technology

Delft Center for Systems and Control

Analysis of engineering wake model validation and calibration with historical data from OWEZ wind farm

Master of Science Thesis

J.A. Keim

January 11, 2024

Student number:	4684214	
Project duration:	February 27, 2023 – Jan 19, 2024	
Thesis supervisor:	Prof.dr.ir. J.W. Van Wingerden	TU Delft
Company supervisors:	Dr.ir. B.M. Doekemeijer	Shell, daily supervisor
	Dr.ir. J.J. Kreeft	Shell, senior advisor

MSc Systems and Control · Faculty of Mechanical, Maritime and Materials Engineering (3mE) · Delft University of Technology

The work in this Master Thesis was supported by Shell Global Solutions International B.V.. Their cooperation is hereby gratefully acknowledged.

Copyright © Delft Center for Systems and Control (DCSC)
All rights reserved.

Acknowledgements

Over the past year, I have not only learned a lot about the world of wake modelling but also really enjoyed academic research and working on my thesis. This experience would not have been the same without the people I worked with during this project.

Firstly, I would like to thank Jan-Willem van Wingerden for his supportive guidance. His feedback and critical questions during our meetings ensured that I was on the right track. Additionally, I am grateful to Jan-Willem for connecting me with my Shell supervisors, Bart Doekemeijer and Jasper Kreeft, who have played an important role in my experience during this thesis.

Secondly, I want to thank Bart for the countless insightful meetings and conversations on the content of my thesis. I really enjoyed our in-depth discussions on FLORIS, validation and the use of engineering wake models. Moreover, his detailed feedback on my drafts taught me to have a critical view and significantly improved my academic writing skills.

Thirdly, I want to thank Jasper. With your involvement, I had the benefit of having not just two, but three supervisors. I am very grateful for your active engagement and support. Our sessions on the physics behind different wake models have been invaluable to my work.

Fourthly, I want to thank Marcus Becker, not only for being my committee member but also for hosting the valuable bi-weekly master meetings with my fellow students. Also, our one-on-one meeting offered new perspectives on dynamic wake modelling and calibration.

Fifthly, I want to thank Wei Yu, for taking the time to be my final committee member. I look forward to meeting you and discussing my work with you.

Finally, I want to thank my friends and family for supporting me in my hard work the past year and, of course, for patiently listening to my endless stories about wind turbines and wakes.

Rotterdam,
January 11, 2024

Julienne Keim

Abstract

Wind turbines are often placed together in wind farms for economic considerations. This causes wake interactions between turbines, resulting in significant power losses. Models that predict these wake losses are critical for estimating wind farm power output and developing strategies to mitigate the wake effect, such as wind farm control. For these applications, engineering wake models are favoured for their computational efficiency. Hence, the validation and improvement of these models is an ongoing area of research. Currently, consensus on the accuracy of engineering wake models is absent in the literature. Existing studies employ varying validation strategies that impact the perceived model accuracy. Furthermore, proposed model improvements often lack quantitative evaluation, limiting the generalisability of the results. Additionally, the potential benefits of calibrating wake model parameters are recognised, yet research on calibration methods and the impact thereof is limited.

This thesis addresses this scientific gap by proposing a holistic framework for the validation and calibration of engineering wake models. The framework combines best practices from literature. First, it accounts for wind direction uncertainty in historical wind farm data. Additionally, it corrects model inputs by including heterogeneous inflow wind speeds. Finally, it offers a methodology for parameter calibration to improve the model's accuracy using historical wind farm data. The overarching framework employs both quantitative and qualitative validation methods to mitigate the impact of experiment design and enable a thorough evaluation of model improvements. The effectiveness of this framework is demonstrated through a case study with SCADA data from OWEZ wind farm and four engineering wake models from the popular control-oriented wake modelling tool FLORIS.

Results show that wind direction uncertainty in SCADA data must be included when validating wake models for specific wind directions or sectors. Additionally, incorporating heterogeneous inflow wind speeds reduced the absolute turbine error by up to 20%. Furthermore, it is demonstrated that calibrating model parameters significantly improves model accuracy. The resulting error reductions reach up to 92% for individual turbines and 65% at farm-level, i.e., for all turbines collectively. Furthermore, results revealed that while the performance of the different models converges post-calibration, differences persist in various scenarios with numerous wake interactions. In these cases, the CC and TurbOPark models outperform the Jensen and GCH models.

Through this holistic framework and the demonstrated potential of model parameter calibration, a path forward is paved for further model improvement in a systematic and quantitative manner.

Table of Contents

Chapter 1

Introduction

Wind energy is becoming an increasingly important energy source, as there is a growing concern regarding climate change [1]. To achieve global Net Zero emissions by 2050, the International Energy Agency (IEA) has specified that 67% of the global energy supply must originate from renewable sources, with wind energy predicted to account for the second largest share [2]. Fortunately, the wind energy supply has grown significantly over the past ten years and, from 2020 onward, is expected to increase its annual capacity four times by 2030 and as much as 15 times by 2050 [2, 3].

To realise this anticipated growth, wind energy generation must have a competitive price [4]. Efforts have been made to lower the Levelised Cost Of Energy (LCOE) through design improvements and better turbine control strategies. This has led to increased overall turbine efficiency and the ability to scale up turbine capacity to a rated power of 15 MW [5].

Grouping turbines in wind farms is another method to reduce the LCOE, due to reduced installation and maintenance costs, land use and environmental impact [6]. However, this leads to challenges caused by the wake interactions between turbines. As a turbine extracts energy from the incoming wind, it alters the flow downstream of the turbine, called a wake. The wake is characterised by a lower wind speed and increased turbulence, resulting in power losses and increased loads on the downstream turbine. The average annual power production losses attributed to the wake effects in wind farms range between 10-20% [7, 8, 9]. It should be noted that the effect of wakes on structural loading is a broad area of research (see, e.g., [10, 11, 12]) and falls outside the scope of this thesis.

Given that wind turbines are often placed in the wake of an upstream turbine, models that predict power losses due to wakes are critical for estimating wind farm power output and developing strategies to mitigate the wake effect, such as wind farm control and layout optimisation [6, 13, 14, 15]. For these applications, engineering wake models are favoured for their computational efficiency. However, this efficiency comes at the expense of relying on heuristics, which often results in model discrepancies. The resulting uncertainty affects both the predicted yield of wind farms and the effectiveness of wake mitigation strategies. Consequently, validating and improving engineering wake models is essential to reduce this uncertainty and is an ongoing area of research.

1-1 Validation of Engineering Wake Models

Engineering wake models have been extensively validated in against historical wind farm data, referred to as Supervisory Control and Data Acquisition (SCADA) data. The process typically involves comparing turbine power capture recorded in historical data to the models' predicted turbine power capture, ensuring identical wind speed and wind direction conditions.

Earlier validation studies focused on gaining an understanding of wake behaviour and wake modelling without providing conclusions regarding the strengths and weaknesses of different models. For instance, Barthelmie et al. [16] compared five wake models to historical data of the larger-scale Horns Rev 1 wind farm, analysing three arrays of 5-8 turbines with varying turbine spacing. They experimented with wind direction bin widths varying from 2° to 30° and concluded that increased bin width and increased turbine spacing both lead to lower observed wake losses. Note that the choice of binning width is a data processing decision, while turbine spacing relates to the physical characteristics of the wake. While one can observe that the models overestimate wake losses for smaller bin widths and were more accurate for larger widths, the study did not conclude on model accuracy. Barthelmie et al. emphasised the need for more research on wind farm wakes.

In a follow-up study, Barthelmie et al. [17] investigated the performance of four wake models on two larger-scale offshore wind farms, Horns Rev 1 and Nysted, for seven different arrays of turbines and wind directions. They used a 5° binning width and quantified model performance by calculating the Root Mean Square Error (RMSE) of turbine power capture. The study concluded better performance for higher wind speeds and for wind directions aligned with the turbine arrays, compared to wind directions that lead to partial wake overlap. Still, Barthelmie et al. highlight significant uncertainties in the accuracy of the current wake models.

Beaucage et al. [18] examined six wake models for arrays of 10 turbines across 30° wind sectors, finding that the engineering wake models underestimate wake losses after 3-4 turbines. Despite figures using a 10° bin width contradicting that statement and indicating an overestimation of wake losses, the overall conclusion was that engineering wake models tend to underestimate wake losses deeper within the turbine array. Such discrepancies highlight the challenges in concluding on model accuracy due to variations in data processing techniques.

Gaumond et al. [19, 20] are among the first to emphasise the effect of binning widths on the validation of wake models, attributing the difference in model performance to wind direction uncertainty in historical data. They point out that this uncertainty arises from factors such as yaw misalignment of turbines relative to incoming wind, spatial variations within the wind farm, and temporal variability in 10-minute averaged historical data. In a follow-up study, Gaumond et al. [20] suggest using a weighted average of simulations of neighbouring wind directions to mitigate this uncertainty, demonstrating a reduced dependence of model accuracy on the chosen binning width.

The findings of these earlier studies are specific to certain flow cases, i.e., wind directions aligned with the turbine arrays [16, 18]. Other research, like Barthelmie et al.'s subsequent work [17], indicate decreased model performance in cases of wind direction slightly misaligned with the turbine arrays. This highlights the dependency of conclusions on experiment design.

The evolution of wake model validation includes focused investigations into model strengths and weaknesses, sometimes leading to the development of new models. For example, Nygaard's series of studies [21, 22, 23, 24, 25] focused on validating and improving wake models for offshore wind farms. Initially, Nygaard [21] assessed the Jensen [26] wake model using data from five large offshore wind farms within a 30° wind direction binning width, finding reasonable accuracy for farms with over 100 turbines. However, the validation was limited to specific turbine arrays aligned with the incoming wind direction. In a subsequent study, Nygaard [22] pointed out that the current validation studies are limited to qualitative validation and specific turbines and lack quantitative metrics to evaluate model improvements. Consequently, he introduced a framework for uncertainty quantification. However, this approach focused on Annual Energy Production (AEP) calculations and does not provide insights into the accuracy on individual turbine level, which is necessary for effective wind farm control. To further improve the accuracy of wake models, Nygaard et al. [24] introduced a new engineering wake model, called Turbulence Optimised Park (TurbOPark). The motivation for developing this new model was recent findings that cluster wakes, i.e. the combined wake behind a wind farm, persist longer than previously assumed [27, 28, 23, 29], which can impact neighbouring farms. These farm-to-farm effects are becoming increasingly important as offshore farms are positioned with an increasing density, e.g., along the European coastlines. The model showed excellent agreement with the data of two upstream turbines and an array of 7 turbines. However, varying binning widths in the study made it challenging to draw conclusions. Furthermore, Nygaard et al. introduced a model for wind farm blockage, i.e., the reduction in inflow wind speed near the centre of the farm, showing slightly improved results. Finally, Nygaard et al. [25] presented another framework for validation and uncertainty quantification, validating both the Jensen model and TurbOPark model to 19 offshore wind farms, with a binning width of 10°. While this study offers quantitative insights, it lacks qualitative analysis to support the model accuracy found. Additionally, it included a heterogeneous background flow and a blockage model but did not quantify their impact on model accuracy, leaving their significance undetermined.

Archer et al. [30] provided a qualitative and quantitative analysis of six engineering wake models on three commercial wind farms: Lillgrund, Nørrekær and Anholt. Their analysis focused on specific turbine arrays using 10° bin widths and single turbines for a 40° range of wind directions with 2.5° bin widths. Overall, they found an underestimation of wake losses. The best performance was seen for Anholt and the worst for Lillgrund. Accordingly, they conclude that the models perform poorer on densely spaced wind farms. The authors find that for wind directions that lead to non-aligned wakes, all six wake models perform worse on the inner turbines. They argued that this is possibly related to the wake superpositioning method[1] used. This study supports its qualitative findings with a quantitative analysis, delivering substantive conclusions. Yet, it falls short in offering an overview of model performance for the entire wind farm, an essential element for model comparison in yield estimations.

Hamilton et al. [15] validated several combinations of velocity deficit, wake-added turbulence and wake superposition methods on the Lillgrund wind farm. Their analysis, both qualitative and quantitative, covered wind directions between 120° and 300° using a 5° binning width. This approach allowed for insights across a range of wind directions, not just specific aligned arrays. They observed that certain wake superpositioning methods and wake-added

[1]The wake models model a single wake, and their cumulative effect is determined by the wake superpositioning method.

turbulence models perform well in scenarios with full wake overlap, whereas others excelled in cases with partial wake overlap. This reveals discrepancies in current methods and models and highlights the need for a validation framework that spans various wind directions.

Doekemeijer et al. [31] compared the Gaussian-Curl-Hybrid (GCH) model, a popular engineering wake model in literature based on the Gaussian wake model by Bastankhah and Porté-Agel [32], to data from three offshore wind farms, including Anholt, OWEZ, and Westermost Rough. Similar to Hamilton et al., Doekemeijer et al. showed performance over a range of wind directions, mitigating the sensitivity to specific wind directions. Moreover, Doekemeijer et al. highlighted the impact of wind direction binning width on validation. They noted that while smaller binning widths are subject to larger uncertainties in the data, they are necessary to evaluate the modelling of a single wake, a key aspect for wind farm control. To address this, Doekemeijer et al. validated for a binning width of 3° as well as 30° degrees. Moreover, they applied a weighted average of simulations of neighbouring wind directions to account for wind direction uncertainty in the historical data, similar to Gaumond et al. [20]. They observed good overall model agreement but, like Archer et al. [30], identified an underestimation of wake losses within the farm, likely due to deep array effects. The study also incorporated heterogeneous inflow wind speeds to account for cluster wakes, wind farm blockage, and coastal effects. While heterogeneity was noted at upstream turbines, it did not significantly improve results compared to a homogeneous inflow. Future research was suggested to investigate these aspects. The study offers valuable insights but lacks quantification of model accuracy and of the impact of wind direction variability or heterogeneous wind speed inflow, limiting its ability to draw substantial conclusions.

Finally, to address the deep array effects mentioned by Doekemeijer et al. [31], Bay et al. [33] carried out a subsequent study in which they validated the Cumulative-Curl (CC) model introduced by Bastankhah et al. [34]. The model, which is based on the GCH model, but incorporates a different near-wake model and novel wake superpositioning method. The authors have tested their model using both a high-fidelity simulation and SCADA data from Anholt, OWEZ, and Westermost Rough. They conclude that the CC model accurately predicts the energy ratio in situations with more wake interactions, such as deep in the array and situations of non-alignment. However, the model improvement found is solely based on a qualitative analysis and occasionally shows decreased performance. Therefore, a quantitative analysis is necessary to support the suggested increase in model accuracy.

1-2 Calibration of Model Parameters

Typically, engineering wake models included literature-recommended parameter values during validation [15, 17, 24, 31]. While several authors highlight the possible benefit of calibrating model parameters [15, 31], research on the topic remains limited. Among the few, Schreiber et al. [35] developed a method to improve engineering wake models by learning from SCADA data. However, rather than simply calibrating existing wake model parameters, they introduced new parameters to account for the unmodelled physics, such as a heterogeneous inflow. This approach of simultaneously optimising both the model input and wake estimation complicates the ability to draw generalised conclusions from the results. Campagnolo et al. [36] addressed this complication by separating the additional parameters in vectors related to different model aspects, including wake model parameters and heterogeneous inflows. While the

wake model parameters changed after calibration, the largest impact was found by introducing a heterogeneous inflow. Yet, due to the experimental setup involving only three turbines in a wind tunnel, the applicability of these findings at a farm level is uncertain.

Calibrating model parameters is more common in the context of wind farm control (e.g., [37, 38, 39, 40]). Yet, as the results are only shown after parameter calibration, the effect on model accuracy can not be concluded. An exception is the study by Van Beek et al. [41]. They calibrated wake model parameters to SCADA data of the Lillgrund wind farm under regular operation, i.e., no wake steering, in preparation for a wake steering simulation. While Van Beek et al. achieved a significant reduction in error for all individual turbines, they developed specific parameters for each wind speed and direction combination, making it challenging to generalise conclusions on optimal parameter values.

1-3 Validation and Calibration Tools

Among these validation and calibration studies conducted, the control-oriented modelling tool FLOw Redirection and Induction in Steady State (FLORIS) has gained popularity. Various studies have employed FLORIS for model validation studies (e.g., [15, 31, 33, 42]), calibration studies (e.g., [36, 41]), wind farm control simulations or experiments (e.g., [37, 38, 39, 43, 44, 45, 46]) and layout optimisation studies (e.g., [47, 48]).

1-4 Research Gap and Research Question

Reflecting on these findings, consensus on the accuracy of engineering wake models cannot be concluded, primarily due to varying validation strategies and their impact on perceived model accuracy. Current literature often limits model validation to specific flow cases [16, 18, 19, 21, 24]. This approach is problematic as research has shown that model performance is scenario-dependent. Different wind directions, leading to either full or partial wake overlap, can significantly influence the accuracy of the models [15, 17, 30, 31, 33]. Additionally, the effect of wind direction uncertainty in historical data is identified, and solutions have been proposed [20, 31]. However, its implementation is not yet standard practice. Furthermore, the role of inflow heterogeneity on model accuracy is another aspect that has gained attention. However, the implications of this factor are either not explicitly demonstrated [24, 25], remain inconclusive [31], or are examined only in the context of single turbines [36]. Consequently, it remains unclear whether its incorporation is essential and, if so, how it should be effectively implemented. Similarly, when introducing new models, the demonstration of their advantages is often either only qualitative [24, 33] or, when quantified, [25] it is done at farm level, i.e., cumulative turbine performance, which limits the ability to evaluate their performance for a single turbine—a critical aspect for effective wind farm control and layout optimisation. In general, a trend in the literature is the emphasis on qualitative analysis over quantitative validation. Such an approach poses significant challenges to systematically comparing different models and studies. In cases where quantitative validation is conducted [15, 22, 25], they are frequently limited to the farm level. Finally, while the potential benefits of model parameter calibration are recognised in several studies [35, 36, 41], there is a gap in research on the development of optimal calibration methodologies and their impact on model accuracy.

The gaps in the current literature mentioned above lead to the formulation of the following research question:

How can the reliability of the current engineering wake models be holistically validated for different model applications, and how can reliability be improved by including inflow heterogeneity or parameter calibration?

To answer this question, this thesis proposes a new validation and calibration framework to improve the accuracy of engineering wake models. This framework addresses common model discrepancies by combining the state-of-the-art methodology to improve both the model input and the model parameters. First, it accounts for wind direction uncertainty in the SCADA data to ensure a fair comparison with the data. Next, it corrects the model input by including heterogeneous input wind speeds. Finally, it calibrates model parameters to improve the wake estimation capabilities of the models. In addition to these steps, this framework introduces new quantitative metrics to validate and improve accuracy both on turbine- and farm-level, providing insight into the effectiveness of each step in the framework and the insights necessary for both yield calculations and farm optimisation through layout optimisation and wind farm flow control. To demonstrate the use of the validation and calibration framework, a case study is conducted with four engineering wake models and historical data from Offshore Windpark Egmond aan Zee (OWEZ) wind farm. The overarching goal of this thesis is to improve the ongoing efforts to enhance the accuracy and reliability of engineering wake models.

1-5 Report Structure

The structure of the thesis is as follows: First, chapter 2 provides an introduction to engineering wake models and an overview of the models from FLORIS employed in this thesis. Second, chapter 3 introduces the OWEZ wind farm to which the models are validated and calibrated, the data pre-processing steps and an analysis of the data of nearby meteorological mast. Third, the proposed validation and calibration framework that is used to improve the models and assess their accuracy is presented in chapter 4. Fourth, a case study with historical data from OWEZ wind farm is presented in chapter 5, providing a qualitative and quantitative assessment of validation and calibration steps, as well as an analysis of the remaining model discrepancies and differences between the models. Finally, chapter 6 summarises the main conclusion from this thesis and provides recommendations for further research.

Chapter 2

Engineering Wake Models

In this thesis, four engineering wake models are compared and calibrated to historical wind farm data. The wake-modelling software used is FLOw Redirection and Induction in Steady State (FLORIS), of which the popularity has steadily risen in recent years. FLORIS [49] is an open-source control-oriented wind farm simulation tool developed by National Renewable Energy Laboratory (NREL), TU Delft and CU Boulder, and maintained by NREL. FLORIS contains several computationally inexpensive steady-state wake models, categorised into the following submodels[1]: wake *velocity deficit model* describing the velocity deficit in a single wake, *wake-added turbulence model* representing the turbulence in the wake and the *wake superposition method* to account for the effect of the upstream turbine's wake on the downstream turbine. This chapter first discusses the assumptions made in engineering wake models and their effect on the applicability of the models in section 2-1. Next, section 2-2 outlines an overview of the wake models analysed in this thesis. Finally, a systematic overview is presented in section 2-3.

2-1 Applicability of Engineering Wake Models

Engineering wake models are considered steady-state models, meaning that the models assume the flow does not change over time and has reached an equilibrium in the farm. Essentially, it means that the models calculate the long-term mean wake behaviour for steady-state, i.e., constant, model inputs. These assumptions are valid for calculations spanning a longer time period, such as Annual Energy Production (AEP) calculations. When engineering wake models are used to develop control and layout optimisation strategies, these assumptions imply that the results are based on steady-state flow conditions. Whether the gained benefit of wind farm control strategies using dynamic flow models is higher is an active topic of research and is outside the scope of this thesis (see, e.g., [50]).

[1] Additionally, several *wake deflection models* are included. However, since this thesis only investigates turbines in regular operation, i.e., no wake steering, the wake deflection models will not be discussed.

2-2 Engineering Wake Models in FLORIS

This section introduces four models from FLORIS that are analysed in this thesis. Note that these models are also partially available in other wake modelling software such as PyWake [51].

2-2-1 Jensen

The Jensen model [52] is one of the oldest and most widely adopted wake models [53]. The velocity deficit in the wake is modelled in accordance with the conservation of mass and assumes a uniform stream-wise velocity. These velocity models are also referred to as top-hat models, due to the distinctive shape of the velocity profile. The velocity deficit in the wake is expressed as a function of the distance behind the rotor using the following equations:

$$1 - \frac{U_w(x)}{U_\infty} = \left(1 - \sqrt{1 - C_T(U_\infty)}\right)\left(\frac{D}{D_w(x)}\right)^2, \tag{2-1a}$$

$$\frac{D_w(x)}{D} = 1 + we\left(\frac{x}{D}\right). \tag{2-1b}$$

In these equations, U_w denotes the wind speed in the wake at a distance behind the rotor x, U_∞ the ambient wind speed, $C_T(U_\infty)$ the thrust coefficient of the turbine, which is a function of the incoming wind speed U_∞, D represents the rotor diameter, and D_w is the wake diameter, a function of x. The wake expansion coefficient we is an empirically determined parameter typically set to 0.03 - 0.05 for offshore applications [16]. This parameter leads to linear wake expansion. The Jensen model is coupled with the Sum of Squares superpositioning method by Katic et al. [26], commonly known as the Park model [26].

2-2-2 Gaussian-Curl-Hybrid

The Gaussian model is based on the observation that the long-term mean velocity deficit in the far wake obtains not a top-hat but a Gaussian shape [54, 55, 56]. The model applies the conservation of mass and momentum and assumes a self-similar Gaussian profile for the velocity deficit. This self-similarity implies that the shape of the Gaussian distribution remains constant as the wake scales. The Gaussian profile accounts for both axial and radial velocity gradients. Consequently, the velocity deficit is a function of the distance behind the rotor x and the radial position r:

$$1 - \frac{U_w(x)}{U_\infty} = (1 - C(x))\exp\left(-\frac{1}{2}\left(\frac{r}{\sigma_w(x)}\right)^2\right), C(x) = \sqrt{1 - \frac{C_T(U_\infty)}{2}\left(\frac{D}{2\sigma_w(x)}\right)^2}, \tag{2-2a}$$

$$\frac{\sigma_w(x)}{D} = \epsilon + k\left(\frac{x}{D}\right), k = k_a I_{\mathrm{CH}}(x) + k_b. \tag{2-2b}$$

In these equations, the Gaussian distribution of the wake width is defined by σ_w, which is a function of x. The wake expansion is defined by the wake expansion coefficient k, which is a function of the turbulence intensity at the rotor $I_{\mathrm{CH}}(x)$ and two tuning parameters k_a and k_b. The default values for k_a and k_b in FLORIS are 0.38 and 0.004, respectively. $I_{\mathrm{CH}}(x)$ is

determined by the Crespo-Hernandez turbulence model [57], which has an empirically derived formula for the near and far wake. The introduction of $I_{\text{CH}}(x)$ in the wake expansion coefficient results in a non-linear wake expansion.

The Gaussian-Curl-Hybrid (GCH) model combines the velocity deficit model by Bastankhah and Porté-Agel [58] and Niayifar and Porté-Agel [59], the wake deflection model by Martínez [60], and the secondary steering model from King et al. [61]. In scenarios without wake steering, GCH falls back to the Gaussian model proposed by Bastankhah and Porté-Agel, and Niayifar and Porté-Agel. In FLORIS GCH is coupled to the Sum of Squares superpositioning method[2].

2-2-3 Cumulative-Curl

In literature, the underestimation of wake losses deeper in the farm is often attributed to the superpositioning method employed. Motivated this discrepancy in existing wake models, the Cumulative-Curl (CC) model [33] builds on the GCH model but replaces the Sum of Squares wake superposition method with derivations based on the Navier-Stokes equations (NS equations) as described by Bastankhah et al. [34]. Additionally, it incorporates Blondel's super-Gaussian velocity deficit model [63] that evolves from a top-hat shape in the near wake to a Gaussian shape in the far wake, which is more consistent with observations. The improvement of the near-wake is more likely to be observed in densely spaced wind farms. The wake velocity deficit is governed by the following equations:

$$1 - \frac{U_w(x)}{U_\infty} = 1 - C_n \exp\left(-\frac{1}{2}\frac{r^m}{\sigma_w^2(x)}\right), C_n = \left(1 - \sum_{i=1}^{n-1} \lambda_{ni}\frac{C_i}{U_\infty}\right) f(C_T(U_\infty)), \tag{2-3a}$$

$$\frac{\sigma_w(x)}{D} = \epsilon + k\left(\frac{x}{D}\right), k = a_s I_{\text{CH}}(x) + b_s. \tag{2-3b}$$

Here, the CC model incorporates a superpositioning method in Equation 2-3a, where C_n considers wakes of upstream turbines on turbine n by the term $\sum_{i=1}^{n-1} \lambda_{ni}\frac{C_i}{U_\infty}$. Additionally, the second part of the equations includes a dependence on the $C_T(U_\infty)$[3], similar to other wake models. Additionally, the Super-Gaussian model is defined by the exponent m, which varies as a function of x. This leads to a higher m near the rotor, creating a top-hat shape, and a lower m downstream, yielding a Gaussian-shaped wake. Similar to the GCH model in Equation 2-2b, the wake expansion in Equation 2-3b is defined by the wake expansion coefficient k, similar to GCH, where tuning parameters k_a and k_b are now denoted as a_s and b_s. The default values for a_s and b_s, based on LES data, are 0.179 and 0.012, respectively.

2-2-4 Turbulence Optimised Park

Similar to the CC model, the development of Turbulence Optimised Park (TurbOPark) is motivated by the underestimation of wake losses deeper in the farm [24]. To address this,

[2]Here it deviates from the description proposed by Niayifar and Porté-Agel [59] using a Linear superpositioning method by Lissaman [62].

[3]For the full set of equations, see [33].

TurbOPark, initially an extension of the Park model, proposes a non-linear wake expansion rate that leads to a fast wake expansion near the rotor and slower further downstream, resulting in longer and smaller wakes. A subsequent version of TurbOPark replaces the Jensen velocity deficit model with a Gaussian-shaped deficit. This updated model, detailed in [25, 64], is implemented in FLORIS and has the following governing equations:

$$1 - \frac{U_w(x)}{U_\infty} = 1 - C(x) \exp\left(-\frac{1}{2}\left(\frac{r}{\sigma_w(x)}\right)^2\right), C(x) = \sqrt{1 - \frac{C_T(U_\infty)}{2}\left(\frac{D}{2\sigma_w(x)}\right)^2}, \quad \text{(2-4a)}$$

$$\frac{d\sigma_w(x)}{dx} = AI(x), I(x) = \sqrt{I_\infty^2 + I_{\text{F}(x)}^2}. \quad \text{(2-4b)}$$

In the given equations, the variables U_w, U_∞, σ_w, D, and x maintain their previously defined meanings. Note that Equation 2-4a is equal to Equation 2-2b from the GCH model. Different to GCH, the wake expansion is governed by the tuning parameter A and turbulence $I_{\text{F}}(x)$. The parameter A is set to a default value of 0.04, established through calibration with data from 19 offshore wind farms [25]. The turbulence intensity $I_{\text{F}}(x)$ is determined using the Frandsen turbulence model [65], which contains an empirical derivation for the turbulence intensity in the near and far wake.

2-3 Overview of FLORIS Models

An overview of the used FLORIS models is presented in Table 2-1. Note that more wake superposition models are available in FLORIS. However, the default superpositioning method of Sum of Squares is used in the remainder of this thesis.

Wake Model	Velocity Deficit	Turbulence Intensity	Wake Superposition
Jensen	Jensen [52, 26]	-	Sum of Squares [26]
GCH	Gaussian [32, 59]	Crespo-Hernandez [57]	Sum of Squares [26]
CC [33]	Super-Gaussian [63]	Crespo-Hernandez [57]	-
TurbOPark [24]	Gaussian [32, 59]	Frandsen [65]	Sum of Squares [26]

Table 2-1: Wake models implemented in FLORIS Version 3.3: Velocity deficit models, turbulence intensity models, and wake superposition methods.

Chapter 3

Data Overview and Pre-Processing

This chapter introduces the data set used to validate and calibrate the wake models in this thesis. First, the available historical wind farm data is detailed in section 3-1. Next, the data pre-processing steps are outlined in section 3-2. Finally, section 3-3 presents an analysis of data from a nearby meteorological mast, offering insights into site-specific atmospheric conditions and a comparison with SCADA measurements.

3-1 Wind Farm Data

The historical data available for this thesis is from the OWEZ wind farm. Figure 3-1a displays its location approximately 10 kilometres off the west coast of the Netherlands and 10 kilometres east of Prinses Amalia Wind Farm. The OWEZ wind farm consists of 36 turbines, with a rated power of 3 MW each, resulting in a cumulative farm capacity of 108 MW. The farm follows a gridded layout as shown in Figure 3-1b, with turbine spacing ranging from 7.2D to 11.1D along the gridded directions. The analysis uses SCADA data from December 2006 to December 2010, available as 10-minute statistics. The SCADA data includes values for time, blade pitch, grid power, wind speed[1], yaw position and Wind Turbine Generator (WTG) availability. Note that the turbines recorded no wind direction. Therefore, the wind direction is assumed to be equal to the yaw angle of each turbine in the remainder of the analysis, aligned with common practice in the literature (see, e.g., [25, 30, 31]).

3-2 Pre-processing of Wind Farm Data

Before validation, the data set is pre-processed to ensure that the data aligns with the scenarios predicted by the wake models, where all turbines operate under regular conditions. This is

[1]Wind speed measurements in the SCADA data have already been translated from anemometer readings at the nacelle to free stream wind speed in front of the turbine.

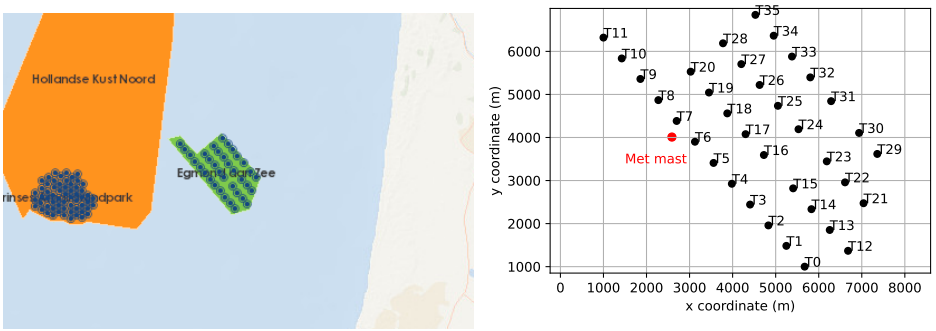

(a) **(b)**

Figure 3-1: Topography of the OWEZ wind farm. **(a)** Geographical location of the OWEZ wind farm in green, with the operational Prinses Amalia wind farm marked in blue dots to the west of the OWEZ wind farm and the non-yet operational Hollandse Kust Noord wind farm in orange. The Dutch coastline lies to the east of the OWEZ wind farm. **(b)** Farm layout consisting of 36 turbines in black. The location of the meteorological mast is shown in red.

crucial because turbines in irregular operation can be mistaken for losses associated with turbine interactions and aligns with common practice in the literature (see, e.g., [15, 25, 31]). The pre-processing steps follow a methodology similar to that outlined by Doekemeijer et al. [31], which can be consulted for a more in-depth explanation. Furthermore, the corresponding codes are documented in the open-source FLASC library [66].

3-2-1 Filtering for Sensor Faults, Turbine Downtime and Irregular Operation

First, the data is filtered to exclude intervals affected by turbine downtime or faulty sensors. Next, power curve outliers, indicating irregular turbine performance, are removed. In addition to the methodology described by Doekemeijer et al., outliers from the pitch angle-wind speed curve are removed to filter for further irregular performance.

3-2-2 Northing Calibration of Wind Direction Measurements

The second step in the data pre-processing involves calibrating wind direction measurements. When using the turbine's yaw angles, a challenge arises as commercial wind turbines rely on relative nacelle misalignment with the wind for yawing, not measurements with respect to the true north. For model validation, wind directions based on the same true north and sign convention for the data and the model are necessary. To address this, the yaw angles of each turbine were calibrated to true north. Note that, in the methodology used, northing calibration is only feasible if the nacelle sensor calibration remains constant throughout the data set. If this is violated, the wind direction of that turbine is categorised as faulty.

3-2-3 Filtering for Affected Turbines

The last step includes removing data points of turbines that interact with faulty turbines. Specifically, if a turbine is inactive, it impacts the power production of downstream turbines,

which affects the validation work. Using the FLORIS models, the influence of the wakes of each turbine on other turbines is computed for each wind direction. Subsequently, data from the affected turbines is also excluded for the corresponding time interval.

3-3 Meteorological Mast Data

Next to the SCADA data, the data from a nearby meteorological mast (met mast) is available. This mast is located approximately 500 metres in front of Turbines 6 and 7, as depicted in Figure 3-1b. The met mast measurements include wind direction, wind speed and wind speed standard deviation, available as 10-minute statistics from July 2005 to December 2010. The measurements are recorded at 70 meters above sea level, equal to the hub height of the turbines. The part of the data collected prior to the wind farm's construction is used to derive the wind climate at the site. The wind rose and turbulence intensity are derived and presented in Figure 3-2. Figure 3-2a reveals a predominant south-west wind direction, typical for the North Sea, and lower wind speeds from the east, possibly influenced by coastal winds. Figure 3-2b displays increased turbulence from the north of 7.8% and an average turbulence intensity of 6.5% across the entire wind rose. Moreover, met mast data contains lower measurement uncertainty than SCADA data. Therefore, the met mast data is compared with the SCADA data. The analysis, detailed in Appendix A, revealed a high standard deviation in the wind direction error and a lower standard deviation in the wind speed error, 13° and 0.9 m/s, respectively. This indicates that even with the northing calibration, uncertainties in wind direction remain. How this is addressed is discussed in section 4-2.

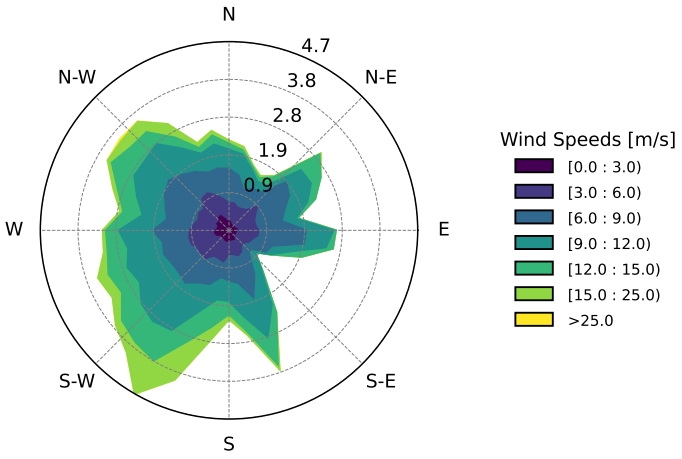

(a) Wind rose showing a predominant wind direction from south-west and lower wind speeds from the east.

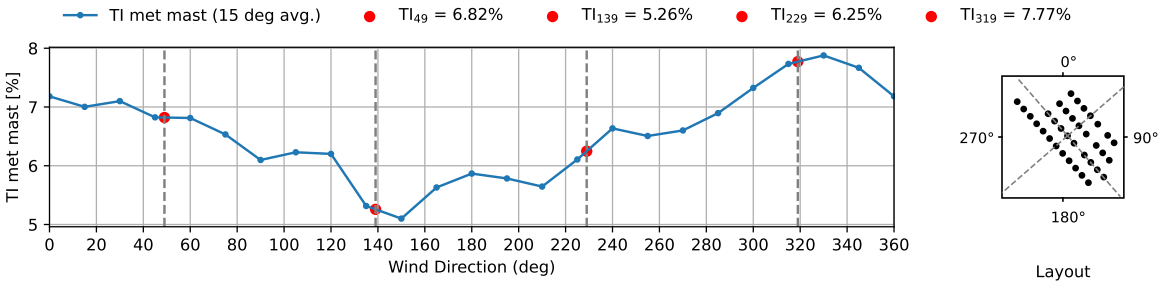

(b) Left: Turbulence intensity averaged in 15-degree wind direction bins for speeds ranging from 4 to 15 m/s, revealing increased turbulence from the north and reduced turbulence from the south. Right: Layout of the OWEZ wind farm, including dashed wind directions.

Figure 3-2: Atmospheric conditions based on the data of a nearby meteorological mast, showing **(a)** Wind rose **(b)** Turbulence intensity

Chapter 4

Model Validation and Calibration Framework

This chapter presents a systematic methodology for validating and calibrating engineering wake models against historical wind farm data. The goal is to validate and improve model accuracy at both the farm and turbine levels. First, the comprehensive validation methodology and designed validation metrics are introduced in section 4-1. Next, the effect of wind direction uncertainty is addressed in SCADA data during validation in section 4-2. Section 4-3 outlines the methodology to correct inflow conditions by including heterogeneous inflow wind speeds. Finally, as a final step in the framework work, a method for calibrating model parameters to improve model accuracy is introduced in section 4-4.

4-1 Validation Metrics and Methods

This section introduces the overarching validation methodology. Subsection 4-1-1 explains the use of the energy ratio metric to compare power output between models and historical data. Subsection 4-1-2 describes the application of this metric in both qualitative and quantitative validation strategies.

4-1-1 Energy Ratio as a Validation Metric

Wake models are typically compared with historical data using a relative power deficit, indicating power capture compared to one or more reference turbines in unwaked conditions. Additionally, several authors introduce a normalised error, standardising the error to power capture or wake loss in the farm (see, e.g., [22], [41], [67]). The latter is primarily helpful for cross-farm accuracy comparisons and, therefore, is not required for this thesis. In this thesis, we apply the energy ratio metric, which quantifies the relative power capture of the selected test turbine(s) — the turbine(s) of interest — relative to the average power capture of

reference turbine(s), which are upstream turbine(s) unaffected by wakes. This methodology aligns with Doekemeijer et al. [31] and is subsequently used by others (see, e.g., [33], [68]).

The energy ratio of test turbine(s) i for a wind direction bin j is calculated as follows:

$$R_{ij} = R(T_i, \theta_j) = \frac{\sum_{k=1}^{K} P_k(T_i, \theta_j)}{\sum_{k=1}^{K} P_k(T_{\text{ref}}, \theta_j)}. \tag{4-1}$$

In this equation,

- $P_k(T_i, \theta_j) \in \mathbb{R}^T$ represents the k^{th} power measurement of test turbine(s) i for wind direction bin j. Here, T denotes the total number of measurements for turbine(s) i. If multiple test turbines are selected, $P_k(T_i, \theta_j)$ is defined as the average power production of all test turbines. However, in this thesis, unless specified otherwise, T_i is considered a single turbine.
- $P_k(T_{\text{ref}}, \theta_j) \in \mathbb{R}^R$ denotes the k^{th} power measurement of the reference turbine(s) under the same wind direction bin j. The total number of measurements for the reference turbines(s) are denoted by R. The reference power $P_k(T_{\text{ref}}, \theta_j)$ is defined as the average power production of the five closest upstream turbines of T_i in a specific radius, in this thesis, set to 5 km.
- K represents the count of measurements that both the test and reference turbines share, defined by $T \cap R$.

Additionally, it is important to highlight that the energy ratio, in its process of summing all measurements, effectively sums over wind speed. Because most wake losses occur when turbines operate below rated power, only time steps where the reference turbine's wind speeds are in the range of 4-15 m/s have been included. For the same reason, this is the most significant range for wind farm control and layout optimisation. Beyond 15 m/s, turbines operate at rated power, resulting in fewer wake losses and often correlates with improved model accuracy. Furthermore, the wind direction binning width is set to 5°. This is small enough to show the profile of a single wake, which is estimated to be 10°-15° [17], and large enough to account for a part of the uncertainty in the SCADA data. Note that the energy ratio represents an average for each wind direction bin. Consequently, more frequently occurring wind directions do not carry additional weight. Finally, it is important to note that due to the specified wind speed range and balanced wind direction weighting, this analysis does not directly reflect the accuracy of the AEP, which is expected to be higher when higher wind speeds are included.

4-1-2 Qualitative and Quantitative Methods for Comprehensive Validation

Chapter 1 highlighted that literature shows contradicting statements regarding model accuracy depending on experiment design. Moreover, assessing the effect of different validation steps and model improvements is challenging due to the lack of quantification in existing studies. Consequently, this thesis aims to provide a comprehensive analysis, employing qualitative and quantitative validation strategies.

Firstly, the qualitative analysis follows the approach outlined by Doekemeijer et al. [31], using two types of figures: The first examines energy ratio curves for specific turbines to analyse individual turbine performance across the entire wind rose. The second evaluates the energy ratios along an array of turbines for a specific wind direction to study wake propagation within the wind farm. This approach enables comparison for both situations where full and partial wake overlap, addressing common engineering wake model discrepancies mentioned in the literature [30, 15].

Secondly, quantitative validation is included to effectively compare models and quantify the effect of different validation steps and model adaptations. This thesis proposes three quantitative metrics for farm and turbine accuracy:

- The **Farm Error** (Equation 4-2) is the most important metric for yield calculations, assessing cumulative wake loss of all turbines. The metric quantifies the percentage mismatch in total energy production between observed data and the model summed across all turbines and wind directions:

$$\text{Farm Error} = \frac{1}{N}\sum_{i=1}^{N}\left(\overline{R}_i^{\text{SCADA}} - \overline{R}_i^{\text{model}}\right), \tag{4-2a}$$

$$\text{where } \overline{R}_i = \sum_{j=1}^{M} R(T_i, \theta_j). \tag{4-2b}$$

  Here, N represents the total number of turbines, T_i denotes turbine number i and $\overline{R}_i$ is the energy ratio as defined in Equation 4-1 for turbine i, aggregated across all M wind direction bins.

- The **Mean Absolute Turbine Error** (Equation 4-3) focuses on individual turbine performance. This information is important for evaluating the suitability of models for wind farm control and layout optimisation, where accurate modelling of individual turbines is essential. To assess individual turbine performance, the metric avoids the cancellation of over- and underestimations among different turbines by taking the absolute value.

$$\text{Mean Absolute Turbine Error} = \frac{1}{N}\sum_{i=1}^{N}\left|\overline{R}_i^{\text{SCADA}} - \overline{R}_i^{\text{model}}\right|. \tag{4-3}$$

- The **Mean Turbine RMSE** (Equation 4-4) provides additional insights into the variation of errors within the wind rose, a perspective not covered by the Mean Absolute Turbine Error. Additionally, this metric is affected by how well the wake width of individual wakes is estimated, an important aspect for applications such as controller design and layout optimisation.

$$\text{Mean Turbine RMSE} = \frac{1}{N}\sum_{i=1}^{N}\sqrt{\frac{1}{M}\sum_{j=1}^{M}\left(R_{ij}^{\text{SCADA}} - R_{ij}^{\text{model}}\right)^2}. \tag{4-4}$$

The qualitative and quantitative validation methods outlined above, using the energy ratio metric, form the core of the validation methodology. The following sections will expand on the steps within the framework designed to ensure fair validation with historical data and improve model accuracy.

4-2 Addressing Wind Direction Uncertainty in SCADA data

When validating against historical data, accounting for uncertainty in the SCADA data is important. Theoretically, the spread of the wake in steady-state models should equal the long-term mean wake for a specific mean wind direction, as outlined in section 2-1. Consequently, it already accounts for temporal variability in the 10-minute averaged wind direction data. However, additional variability may arise from measurement noise and yaw hysteresis, i.e., the turbine's delayed response to changing wind directions. This additional variability in the SCADA data leads to the wake loss being spread over a broader range of wind directions in the data. This has no effect when validating for the Farm Error or Turbine Error, as the metrics are summed over all wind directions. However, when investigating the accuracy for specific wind directions, this impacts our validation where wake models tend to show shallower wakes than observed in SCADA data.

To address this, Doekemeijer et al. [31] apply a Gaussian distribution with a standard deviation of 3° on the wind direction input of the wake models, denoted as σ_{wd}. The reasoning behind selecting this value for σ_{wd} is neither clearly defined nor validated[1]. Therefore, this thesis defines the σ_{wd} as representing the additional wake spread due to uncertainty in the SCADA data. Moreover, this parameter is calibrated to historical data to derive an appropriate value. To do so, this thesis adopts a solution inspired by the methodology of Doekemeijer et al. [31]. Instead of applying a Gaussian distribution on the wind direction input of FLORIS like Doekemeijer et al., we apply a Gaussian distribution to the turbine power outputs simulated by FLORIS, blending the wake loss across a range of wind directions. The benefit of implementing the uncertainty as a post-processing step is that we can significantly reduce computation time for calibrating the optimal distribution to match the SCADA data. Essentially, this modification increases the width of the wake while preserving the total energy loss in the wake. By accounting for uncertainty in the measurements, we ensure a fair comparison between the data and the wake models.

Calibration Method
Since it is unclear to what extent each model already accounts for measurement uncertainty in their wake width, the value for σ_{wd} will be calibrated for each model independently. The cost function the parameter is calibrated to is the Turbine RMSE as in Equation 4-4, minimising the variation of errors within the wind rose. Note that including a heterogeneous inflow and modifying model parameters affect the cost function for σ_{wd}. Consequently, this value is calibrated as the last step.

[1] According to B.M. Doekemeijer (personal communication, December 2023) "there is an ongoing debate about whether σ_{wd} should be designed only to address the added uncertainty in SCADA measurements or also to account for the variability in wind direction during 10-minute intervals". Such definition affects the reasoning behind the value for σ_{wd}.

4-3 Incorporating Heterogeneous Inflow Wind Speeds

The previous section addressed challenges encountered in validation using SCADA data. This section focuses on wind inflow dynamics, which are often overlooked in the current validation and calibration studies. Namely, most engineering wake models assume a homogeneous wind speed inflow, whereas several studies have identified heterogeneous inflow wind speeds (see, e.g., [23, 25]). Therefore, it is recommended that one models the heterogeneity in the wind inflow when validating and calibrating engineering wake models. FLORIS offers an option to modify inflow conditions by assigning each turbine a wind speed multiplier per wind direction. This thesis uses SCADA data to generate generalised wind speed profiles. The advantage of using SCADA data is that it contains all factors affecting wind inflow, including topography-related background flows, neighbouring wind farms, and global blockage effects, eliminating the need for additional models. A similar methodology could be applied using high-fidelity simulations if no SCADA data is available.

Calibration Method
A generalised wind speed profile is derived from SCADA data, normalising the energy ratios of each upstream turbine to the average of all upstream turbines, similar to Doekemeijer et al. [31]. The normalised energy ratios of the upstream turbines are calculated for 10° wind direction bins to minimise overfitting to the data. The wind speed multiplier is determined by taking the cubic root of the normalised energy ratios, following the turbine power-proportional relationship $P_{\text{turbine}} \propto U_{\infty}^{3}$. Note that the multiplier is assumed to be constant over all wind speeds, indicating a generalised pattern. Next, this profile is extended downstream along the incoming wind direction, advancing the observed gradient over the farm. Based on this gradient, a wind speed multiplier is derived for each turbine, denoted as $H_{\text{ws}_+}(T_i, \theta)$. Next, we interpolate $H_{\text{ws}_+}(T_i, \theta)$ between each 10° average to obtain values for the single wind directions. To implement the derived wind speed heterogeneity, these multiplier values, which vary for each turbine based on the wind direction, are multiplied by the mean incoming wind speed. Note that the derivation of inflow heterogeneity does not involve the use of wake models and is, therefore, the same for all models and not affected by parameter calibration.

4-4 Wake Model Parameter Calibration

Following the implementation of wind speed heterogeneity in the previous section, we focus on improving model characteristics through parameter calibration. By addressing the model inputs first, we ensure a fair comparison with the data and lay the foundation for the calibration process.

Calibration of model parameters fundamentally alters wake characteristics. It influences the total energy loss in the wake and, consequently, the total energy output of the farm. Calibrating the model parameters to SCADA data serves several benefits. First, it analyses the validity of the literature-recommended parameters for the present operational wind farms. Currently, most parameters have been calibrated to high-fidelity simulations or wind tunnels. An exception is the TurbOPark model, which has been calibrated to several offshore wind farms. Second, a similar exercise is expected to be executed before wind farm control is applied to a farm to adjust the models to the specific wind farm. Therefore, it is important to design a robust methodology.

Choice of Wake Model Parameters

The Jensen, GCH, CC, and TurbOPark models contain 1, 4, 6 and 1 tunable wake parameters, respectively. Consequently, the calibration parameter choices for Jensen and TurbOPark are straightforward: we for Jensen (Equation 2-1), representing wake expansion, and A for TurbOPark (Equation 2-4), denoting the wake expansion calibration parameter. In the case of the GCH models, Sobol sensitivity studies indicate that the primary sensitivity lies in k_a (Equation 2-2), governing the impact of TI on wake recovery [41, 68]. No sensitivity studies have been conducted for the CC model; however, as the models partially overlap, the same calibration parameter, a_s (Equation 2-3), weighing the influence of TI in wake recovery, has been chosen for the CC model.

Model	Parameter	Physical representation	Min	Max	Ref.
Jensen	we	Wake expansion	0.01	0.10	0.05
GCH	k_a	Weight of TI in wake expansion	0.10	0.50	0.38
CC	a_s	Weight of TI in wake expansion	0.05	0.30	0.18
TurbOPark	A	Wake expansion calibration	0.01	0.15	0.04

Table 4-1: Calibration parameters along with their physical representations, optimisation bounds and reference values, i.e., the current literature-recommended values.

Calibration Method

In FLORIS, the model parameters can easily be adjusted. To reduce optimisation time, the models have been pre-calculated for a set of values for the parameters outlined in Table 4-1. Given the limited information available in existing literature regarding the calibration of these parameters, the optimisation bounds were derived through a visual analysis of energy ratio curves across various upper and lower bounds. Such a method ensured that the optimal values lay within the determined optimisation bounds. Furthermore, the literature lacks consensus on the best calibration method and cost function, given limited research on calibration. Two different cost functions are explored in this thesis. First, several authors use something similar to the yield error, defined as follows:

$$\Phi^{\text{opt,yield}} = \arg\min_{\Phi} \left(\overline{R}_{\text{w,farm}}^{\text{SCADA}} - \overline{R}_{\text{w,farm}}^{\text{model}(\Phi)} \right), \tag{4-5a}$$

$$\text{where } \overline{R}_{\text{w,farm}} = \overline{R}_{\text{w}}(T_{\text{farm}}). \tag{4-5b}$$

In these equations, Φ^{opt} represents the model parameter that minimises the cost function. The bar in $\overline{R}$ indicates that the energy ratio is summed over all wind directions M as in Equation 4-2b. In R_{w}, the w denotes a weighted energy ratio, where wind directions that are more prevalent in the data set carry more weight. $R_{\text{w}}(T_{\text{farm}})$ represents the weighted energy ratio for all N turbines collectively, where T_i in Equation 4-1 consists of multiple turbines. This method, rather than summing the energy ratios of individual turbines, gives more weight to turbines with higher energy ratios. While this may benefit the accuracy of yield estimations, it could compromise individual turbine performance, which is unfavourable for wind farm control. Therefore, this thesis also explores a second cost function emphasising individual turbine performance, the cumulative absolute turbine error:

$$\Phi^{\text{opt,turb.}} = \arg\min_{\Phi} \frac{1}{N} \sum_{i=1}^{N} \left| \overline{R}_{\text{w},i}^{\text{SCADA}} - \overline{R}_{\text{w},i}^{\text{model}(\Phi)} \right|. \tag{4-6}$$

Similar to Equation 4-5a, the weighted energy ratio $R_{\mathrm{w},i}$ is used. Our training and test sets are not identical because in our validation framework outlined in section 4-1, we use the unweighted energy ratio. An alternative approach involves dividing the data set into a training and test set. However, due to the unequal distribution of uncertainties in the data set, such as seasonal variations, turbine availability and measurement errors, further investigation is necessary to ensure an appropriate data split and falls outside the scope of this thesis.

Chapter 5

Results and Discussions

This chapter provides a case study of the model validation and calibration framework outlined in chapter 4. In this case study, four engineering wake models in FLORIS are analysed. The models are compared to historical data from the OWEZ wind farm, which has undergone several pre-processing steps outlined in chapter 3. This chapter is organised as follows. First, section 5-1 will outline the identified heterogeneity gradients and the calibrated values for the model parameters Φwind direction standard deviation σ_{wd}. Next, we will investigate how different steps in the framework affect the agreement of the models with SCADA in section 5-2. Second, a more detailed analysis of the calibrated models will be provided in section 5-3.

5-1 Calibration Outcomes: Inflow Heterogeneity, Model Parameters, and Wind Direction Standard Deviation

This section presents the results of calibrating the heterogeneous inflow patterns, model parameters (Φ), and the wind direction standard deviation (σ_{wd}).

The heterogeneity maps for the OWEZ wind farm, developed using the methodology in section 4-3, demonstrate gradients indicative of global blockage, coastal effects, and farm-to-farm effects with the neighbouring Prinses Amalia Wind Farm. Further details and corresponding figures can be found in Appendix B.

Following the implementation of a heterogeneous inflow, the parameters Φ and σ_{wd} were calibrated as detailed in section 4-4 and section 4-2, respectively. Table 5-1 presents calibrated values for Φ and σ_{wd}. Investigating the values for $\Phi^{\text{opt,yield.}}$ and $\Phi^{\text{opt,turb.}}$ similar trends can be observed. The results indicate significant parameter changes in the TurbOPark model, which is noteworthy because, within the industry, the model is favoured for its improved wake loss estimations. Another interesting observation is that the parameters of GCH and CC models converge, possibly because they both use similar velocity deficit methods. Lastly, it is worth noting that minimal parameter changes are observed for the CC model. Moreover,

Model	Φ^{ref}	$\Phi^{\text{opt, yield.}}$	$\Phi^{\text{opt, turb.}}$	σ_{wd}
Jensen	0.05	0.042	0.038	4.5°
GCH	0.38	0.237	0.195	4.4°
CC	0.18	0.231	0.174	4.4°
TurbOPark	0.04	0.095	0.077	3.7°

Table 5-1: Calibrated parameters obtained during model optimisation. The table presents the reference parameter before calibration Φ^{ref}, the calibrated model parameters $\Phi^{\text{opt,yield.}}$ and $\Phi^{\text{opt,turb.}}$ corresponding to cost functions Equation 4-5a and Equation 4-6, respectively. For validation, the $\Phi^{\text{opt,turb.}}$ is employed. Consequently, the wind direction standard deviation σ_{wd} is calibrated using models containing $\Phi^{\text{opt,turb.}}$.

the table shows that model parameter calibration outcomes differ based on the chosen cost function, emphasising the importance of aligning the cost function with the intended model application. Therefore, this thesis focuses on the turbine error, aiming to enhance the models for wind farm control experiments. Consequently, the values for σ_{wd} are calibrated to the models containing $\Phi^{\text{opt,turb.}}$. Separate calibrations are performed for the different models, resulting in a σ_{wd} ranging between 3.7° and 4.5°. They are exceeding the recommended 3° in literature [20, 31], indicating the relevance of the (re)calibration of this value.

5-2 Analysing the Impact of Different Steps in the Validation and Calibration Framework

This section investigates the impact of different steps in the validation and calibration framework on model accuracy. The model performance is evaluated before and after the incorporation of:

- wind direction uncertainty,
- heterogeneous inflow wind speed,
- and calibrated model parameters.

In the remainder of this section, subsection 5-2-1 presents the energy ratio curves of two turbines, one at the wind farm's edge and one at the centre. Subsequently, subsection 5-2-2 displays the energy ratios of turbine arrays for specific wind directions, including wind direction aligned and slightly misaligned with the farm layout. In addition to the qualitative analysis, subsection 5-2-3 offers a quantitative overview of the effect of the different steps in the validation and calibration framework.

5-2-1 Single Turbine Analysis

In Figure 5-1, we examine the energy ratio curve of Turbine 28, located in the north-western section of the wind farm, identifying several model discrepancies.

Firstly, in the benchmark evaluation in Figure 5-1a, wind direction variability is evident by sharp wake loss dips in the wake models but shallow dips in the SCADA data. This is

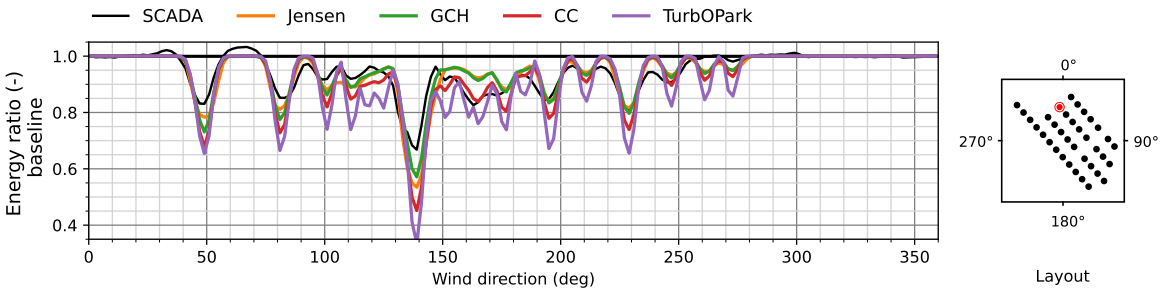

(a) Benchmark evaluation before any additional steps

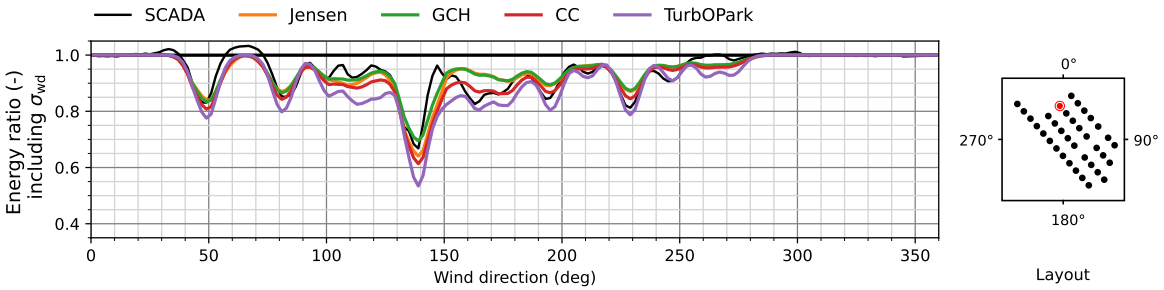

(b) Including wind direction uncertainty (σ_{wd})

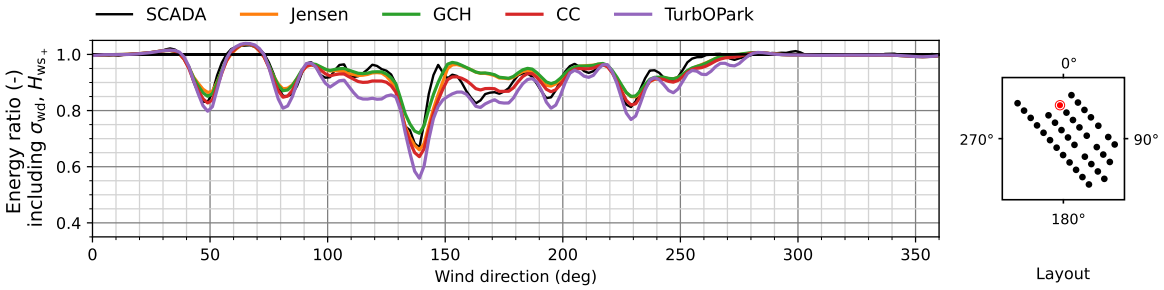

(c) Including wind direction uncertainty (σ_{wd}) and heterogeneous inflow wind speeds (H_{ws_+})

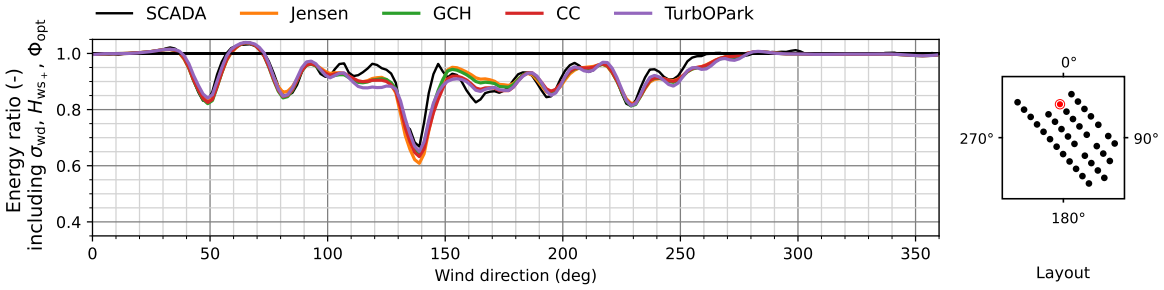

(d) Including wind direction uncertainty (σ_{wd}), heterogeneous inflow wind speeds (H_{ws_+}) and calibrated model parameters (Φ_{opt})

Figure 5-1: Left: Energy ratio curves of Turbine 28 in the OWEZ wind farm for wind directions between 0° and 360°. The subfigures display the model performance by including wind direction uncertainty, heterogeneous inflow wind speeds and calibrated model parameters. Right: Layout of the OWEZ wind farm indicating the location of Turbine 28.

particularly evident in the wind direction range between 200° and 280°. In this sector, Turbine 28 experiences wakes from western Turbines 8, 9, 10, 11 and 20 (shown in Figure 3-1b). For wind directions within this range, all models assume a free stream wind speed between the wakes of these turbines. Conversely, the SCADA data does not distinctly detect wakes from the individual turbines. This discrepancy can be attributed to the models assuming a precise wind direction for the respective wind direction bin. At the same time, the SCADA data is influenced by uncertainty, as discussed in section 4-2. To address this, we introduce a wind direction distribution, σ_{wd}, in Figure 5-1b, leading to an improvement in wake width estimation, particularly noticeable between 200-250°. Secondly, energy ratio values exceeding one indicate that the selected turbine captures more power than the average of the upstream turbines, likely due to heterogeneous wind speed inflow. The heterogeneity in the SCADA data becomes evident at wind directions of 35°, 65°, and 265°. A combination of blockage, coastal effects and the neighbouring Prinses Amalia Wind Farm may explain this effect. Figure 5-1c displays the energy ratio curve incorporating heterogeneous inflow wind speeds, revealing a noticeable improvement for the aforementioned wind directions. Finally, dissimilarity in wake depth between the models and the data persists around 100-190° and in deeper wake losses at locations such as 49°, 80°, and 230°. Here, TurbOPark tends to overestimate, while GCH underestimates wake losses. The incorporation of calibrated model parameters Φ_{opt} in Figure 5-1d addresses this issue, resulting in improved wake depth estimation. Notably, all models show similar behaviour for most wind directions, with noticeable differences for wind directions neighbouring 139°, characterised by partial wake overlap. Despite the improvements found through the additional validation and calibration steps, deviations from the SCADA data persist. Specifically, a difference in wake width remains for 139°, likely due to non-zero-mean wind direction uncertainty in the SCADA data. The underestimation between 100° and 130° may be attributed to coastal winds. Further discussion on these deviations from SCADA data is provided in section 5-3.

The energy ratio curves for Turbine 15, located in the southern centre of the wind farm and surrounded by turbines on all sides, are shown in Figure 5-2. Initially, as seen in Figure 5-2a, all models inaccurately estimate wake depth and width with literature-recommended model settings. These issues are addressed by including wind direction variability and the calibration of model parameters, illustrated by Figure 5-2b and Figure 5-2c, respectively. As Turbine 15 shows minimal effects from inflow heterogeneity, a separate figure is not presented. After all three validation and calibration steps, performance aligns with Turbine 28, where all models demonstrate similar performance for most wind directions. Similar to Figure 5-1d, an overestimation of wake losses is noticeable for eastern wind directions, likely attributed to coastal effects. The models also diverge in performance during instances of multiple-turbine wake interactions (e.g., 5°, 300-310°, 340-350°), resulting in partial wake overlap. A more in-depth analysis of instances of deviation from the SCADA data will be provided in section 5-3.

5-2-2 Turbine Arrays Analysis

While the single turbine analysis provided insights into model performance across the wind rose, it does not fully describe wake propagation throughout the farm. Therefore, this section focuses on specific wind directions to visualise wake propagation within turbine arrays. Two wind directions are examined: first, at 139°, where the layout aligns with the incoming wind, resulting in full wake overlap. Second, at 304°, the wind direction is slightly misaligned

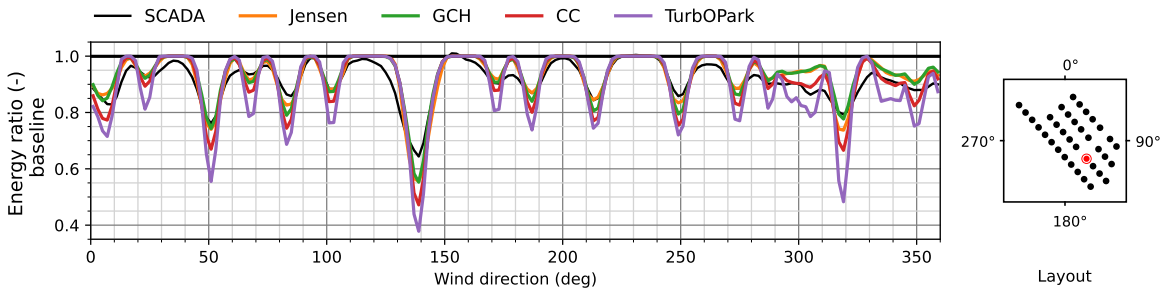

(a) Benchmark evaluation before any additional steps

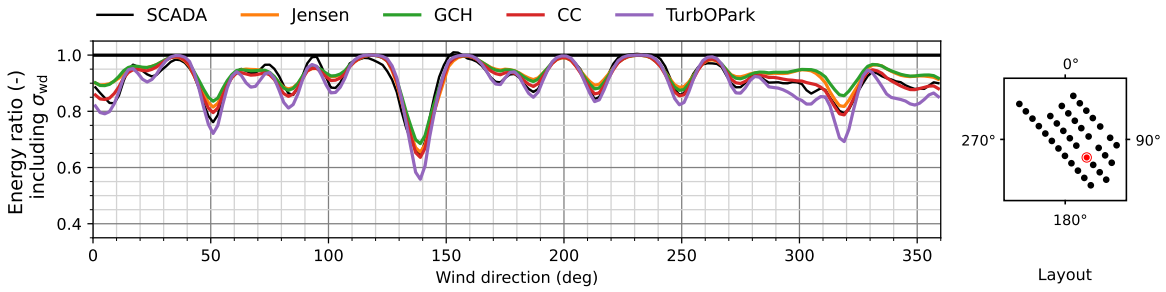

(b) Including wind direction uncertainty (σ_{wd})

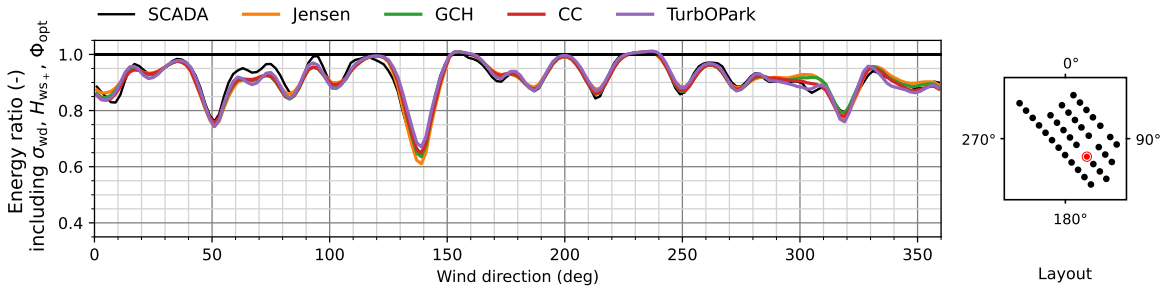

(c) Including wind direction uncertainty (σ_{wd}), heterogeneous inflow wind speeds (H_{ws_+}) and calibrated model parameters (Φ_{opt})

Figure 5-2: Left: Energy ratio curves of Turbine 15 in the OWEZ wind farm for wind directions between 0° and 360°. The subfigures display the model performance by including wind direction uncertainty, heterogeneous inflow wind speeds and calibrated model parameters. As Turbine 15 exhibits minimal effects from inflow heterogeneity, a separate figure is not provided. Right: Layout of the OWEZ wind farm indicating the location of Turbine 15.

with the turbine layout, leading to partial wake overlap. Displayed in Figure 5-3 and 5-4 respectively. The sub-figures in both figures visualise performance after the different steps in the validation and calibration framework. Performance without wind direction uncertainty included is omitted, as its implementation was demonstrated to be essential for a fair comparison for single wind directions in Figure 5-1 and 5-2.

First, in Figure 5-3, the energy ratios of all 36 turbines are shown for a wind direction of 139°, indicating the power capture of each turbine relative to Turbine 0. In the top figure, Figure 5-3a, the SCADA data of other upstream turbines (Turbine 12, 21 and 29) show an energy ratio below one, indicating a heterogeneous wind speed inflow for this wind

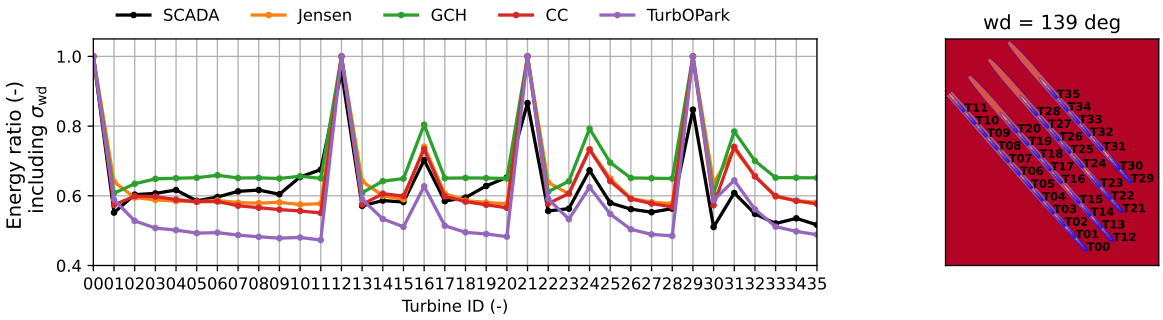

(a) Including wind direction uncertainty (σ_{wd})

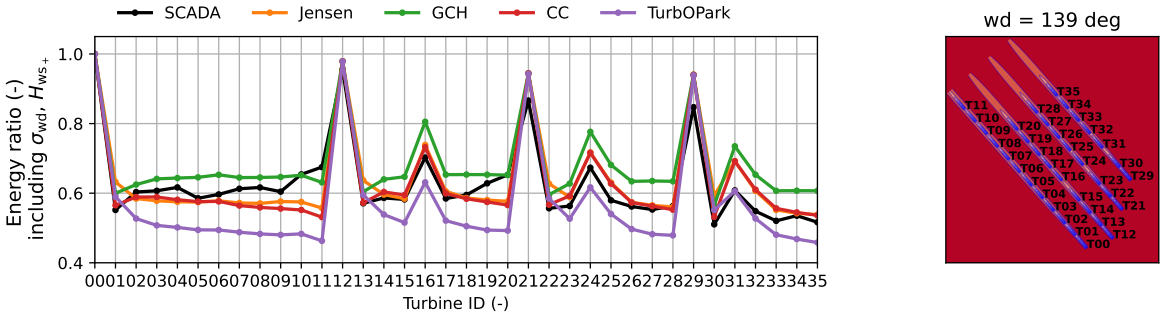

(b) Including wind direction uncertainty (σ_{wd}) and heterogeneous inflow wind speeds (H_{ws_+})

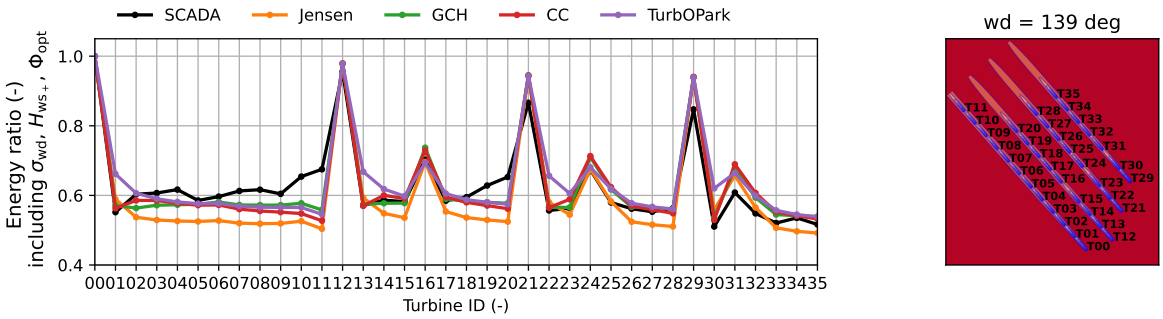

(c) Including wind direction uncertainty (σ_{wd}), calibrated model parameters (Φ_{opt}) and heterogeneous inflow wind speeds (H_{ws_+})

Figure 5-3: Left: Energy ratios of all 36 turbines for a wind direction of 139°, displaying full wake overlap due to alignment of the wind direction with the turbine layout. Subfigures illustrate model validation and calibration steps, including wind direction uncertainty, heterogeneous inflow wind speeds and calibrated model parameters. Right: Flow field visualisation of the OWEZ wind farm for a wind direction of 139° and wind speed of 8 m/s.

direction. The wind speed gradient observed in the SCADA data may be caused by lower wind speeds coming from the coast located east of the wind farm, affecting the turbines positioned further east. In the middle figure, Figure 5-3b, a heterogeneous wind speed gradient across the wind farm is introduced. This enhances the performance of upstream turbines, yet an overestimation of energy ratios persists. This is because the gradient, derived from the SCADA data, is an average of 10-degree wind direction bins rather than the specific wind direction depicted in the figure. Such generalisation is necessary to prevent overfitting. Note

that the effect of heterogeneous inflow is extended beyond upstream turbines, influencing the performance of other turbines in the array, notably in Turbines 29 to 35. The bottom figure, Figure 5-3c, shows the performance after model parameter calibration. Similar to subsection 5-2-1, a convergence of model performance can be found. However, differences remain. Moreover, an overestimation of the energy ratio in the first turbine of the array has a cascading effect, impacting the energy ratios in the entire array. Upon closer examination of the magnitude of the wake losses, it is evident that there is an overall overestimation of wake losses for this wind direction deeper in the array.

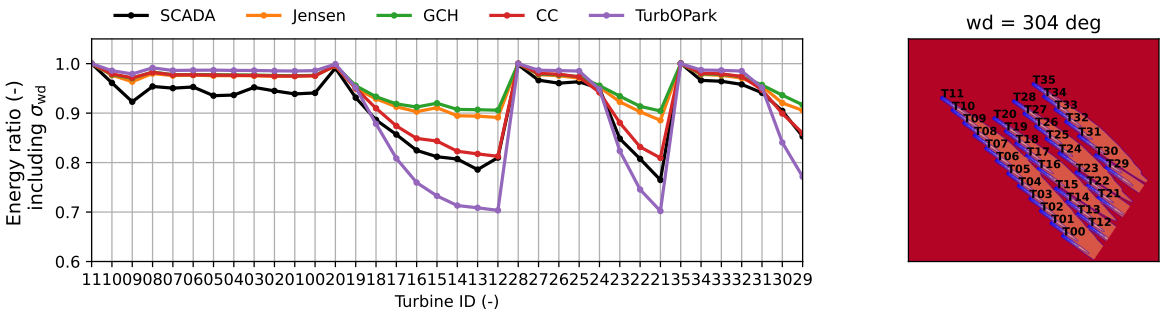

(a) Including wind direction uncertainty (σ_{wd})

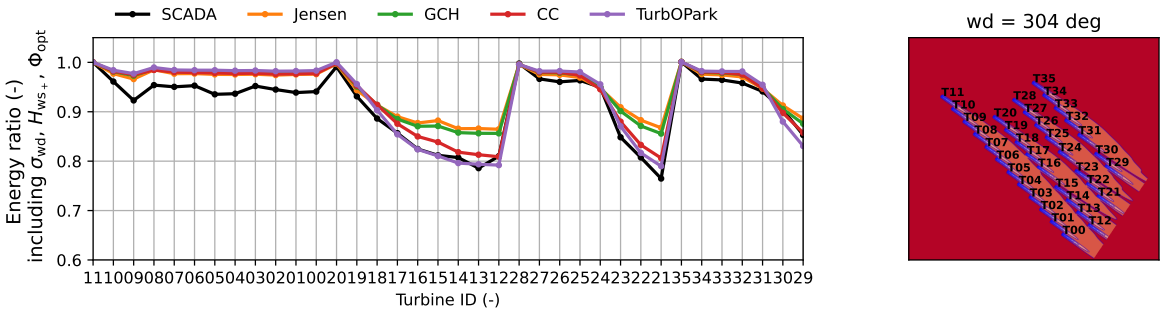

(b) Including wind direction uncertainty (σ_{wd}), heterogeneous inflow wind speeds (H_{ws_+}) and calibrated model parameters (Φ_{opt})

Figure 5-4: Left: Energy ratios of all 36 turbines for a wind direction of 304°, displaying partial wake overlap due to a slight misalignment of the wind direction with the turbine layout. Subfigures illustrate model validation and calibration steps, including wind direction uncertainty, heterogeneous inflow wind speeds and calibrated model parameters. Given the minimal effects of inflow heterogeneity at 304°, a separate figure is omitted. Right: Flow field visualisation of the OWEZ wind farm for a wind direction of 304° and wind speed of 8 m/s.

The energy ratios of the turbine arrays for a wind direction of 304° are shown in Figure 5-4, with the sub-figures displaying the performance after the different steps. As minimal effects from inflow heterogeneity were visible for 304°, a separate subfigure is not presented. Similar to the findings in subsection 5-2-1 and Figure 5-3, significant differences in wake depth are evident between the models before calibration, with convergence occurring post-calibration. It can be observed that the calibration has the most significant impact on the TurbOPark. This was expected after analysing the calibrated model parameters in section 5-1. A more in-depth analysis of the performance of the different models will be provided in section 5-3.

The qualitative analysis has demonstrated that each step in the validation and calibration framework improves the alignment between wind farm data and wake models. The implementation of wind direction uncertainty improved wake width estimation. The heterogeneous inflow wind speeds matched the trends observed in the SCADA data, and models with calibrated wake expansion parameters showed excellent wake loss estimations across most wind directions.

5-2-3 Quantitative Results

The previous subsections illustrated the qualitative performance of the designed validation and calibration framework. This section concludes with a quantitative overview of the improvement in model performance resulting from the different steps. The results are divided into three metrics:

- **Farm Error** (Equation 4-2),
- **Mean Absolute Turbine Error** (Equation 4-3),
- **Mean Turbine RMSE** (Equation 4-4).

For further details on the definition of these metrics, see section 4-1.

Figure 5-5 quantifies the impact of the different model validation and calibration steps on various validation metrics for the different models, providing an overview of the effectiveness of these measures. In the initial row of the bar chart, the effect of the different model validation and calibration steps is evaluated for the Farm Error. The step that significantly impacts the Farm Error is model parameter calibration. This improvement results in a Farm error under 0.34% for all models. Comparing such values to the literature is challenging due to dependence on validation metrics and experiment design. Nonetheless, an analysis of error reduction reveals a significant decrease, ranging from 88-92%[1]. On the other hand, the CC model shows a slight decrease in accuracy. This can be attributed to the different wind direction distribution in the data of the training set. Furthermore, the inclusion of wind direction uncertainty and the heterogeneous inflow wind speeds are expected to have minimal impact on the Farm Error. In the context of including wind direction uncertainty, the total energy loss in the wake remains constant. In the case of heterogeneous inflow, the wind speed gradient applied maintains the same average incoming wind speed. Consequently, both should yield no different results when all turbines and wind directions are summed in the farm error. Nevertheless, a slight change in accuracy is observed. It is unclear why this happens, but it is possibly related to the binning of the wind directions near the 0-360° transition.

Examining the middle row of the bar chart reveals improvements through heterogeneous inflow and parameter calibration. As we are still summing over all wind directions, the inclusion of wind direction uncertainty has minimal impact for reasons equal to those of the Farm Error. Concerning the inclusion of a heterogeneous inflow, a reduction of 3-24% is observed. In theory, including heterogeneous inflow wind speeds should affect all models similarly. Further investigation reveals that, when implementing heterogeneity after calibration, all models show an error reduction of around 20%, similar to CC. Parameter calibration leads to the

[1]Not including CC as its parameter undergoes minimal change.

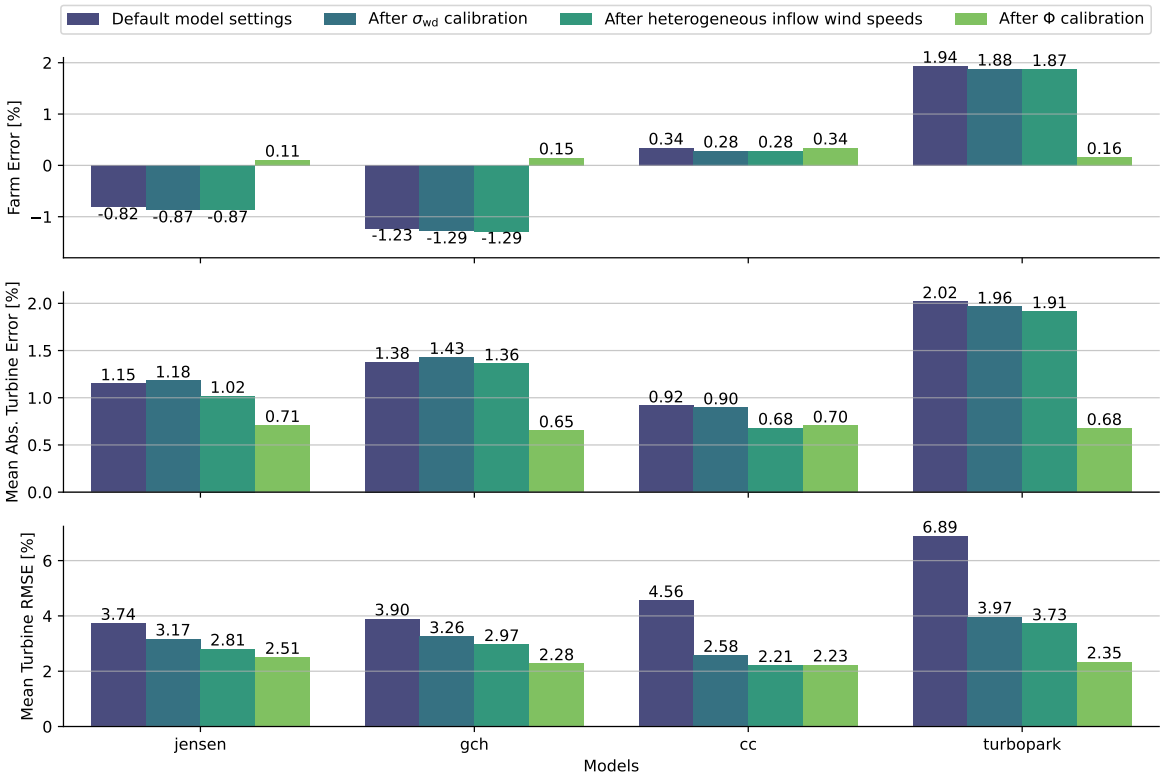

Figure 5-5: Bar chart specifying model performance following various validation and calibration steps. Each row represents a different validation metric: the Farm Error (Equation 4-2), Mean Absolute Turbine Error (Equation 4-3) and Mean Turbine RMSE (Equation 4-4), offering insights into model performance at both farm- and turbine-levels. Each column displays the performance for different models: Jensen, GCH, CC and TurbOPark.

most significant improvements, ranging from 30-65%[1]. This reduction aligns with expectations since the cost function for calibration is the Mean Absolute Turbine Error. Notably, the Jensen model shows a less significant improvement in the Mean Absolute Turbine Error compared to the Farm Error. This suggests that the low Farm Error results from relatively more cancellation of over- and underestimations among turbines compared to other models, indicating incorrect wake predictions.

Finally, looking at the bottom row of the bar chart, the Mean Turbine RMSE is affected by all three steps. First, the improvement found by including wind direction uncertainty is expected as this is the cost function for its optimisation. Second, it shows that including a heterogeneous inflow lowers the error for most wind directions. Third, the reduction in turbine RMSE by calibration is a promising outcome, indicating improved turbine accuracy across most wind directions. This suggests that the improvement found by calibration extends beyond the cost function, and a more fundamental enhancement in performance is achieved by calibration. The model adaptations lower the Mean Turbine RMSE with 15-43%, 6-14% and 10-37%[1], respectively.

[1]Not including CC as its parameter undergoes minimal change.

In conclusion, all three steps substantially impact model accuracy across all models. The results show that parameter calibration has the potential to improve model accuracy, impacting all validation metrics significantly. Furthermore, introducing heterogeneous inflow wind speeds affects the Mean Absolute Turbine Error and Mean Turbine RMSE, impacting validation only on turbine-level. The addition of uncertainty on the wind direction input only improves the Mean Turbine RMSE. In line with the qualitative validations, it can be observed that model performance converges after the calibration steps. The subsequent section will further investigate the origin of the remaining errors and compare the optimised models.

5-3 Analysing the Accuracy of the Enhanced Wake Models

The previous section highlighted the significance of the steps in the proposed validation and calibration framework. In applications such as wind farm control and layout optimisation, where the precision and uncertainty of wake models are crucial for realistic outcomes, deviations from SCADA data require closer examination. This section shows how the framework can be used to investigate instances of model deviation from SCADA data and analyse differences between models, aiming to highlight points of attention and pave the way for model improvement.

5-3-1 Accuracy Along Different Wind Directions

To pinpoint instances where the models show the most significant divergence from the SCADA data, the Farm Error[2] for each wind direction is visualised in Figure 5-6. To highlight wind directions aligned with the farm layout, vertical dashed lines are placed at 49°, 139°, 229°, and 319°. Figure 5-6 shows two notable instances of deviation: a consistent overestimation of wake losses between 50° and 120°, and zig-zag trends around 139° and 319°, which will be discussed next.

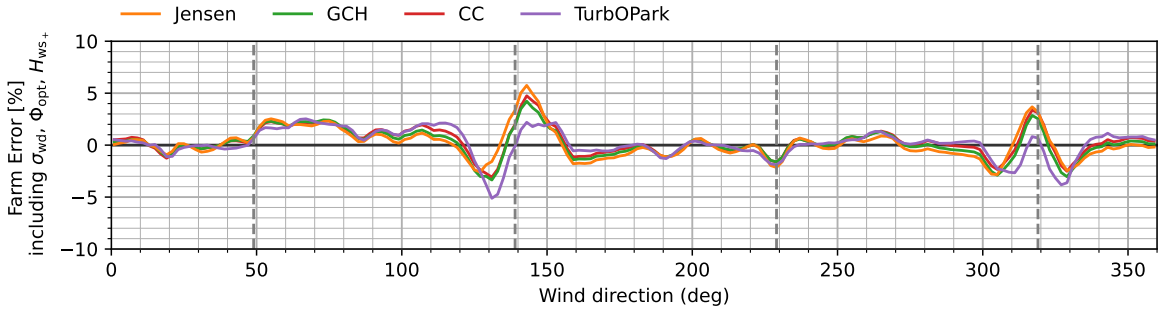

Figure 5-6: Farm Error[2] (Equation 4-2) per wind direction indicating areas where models deviate most from historical data. Vertical dashed lines mark wind directions aligned with the farm layout (49°, 139°, 229°, and 319°). Results are after the inclusion of wind direction uncertainty (σ_{wd}), heterogeneous inflow wind speeds (H_{ws_+}) and calibrated model parameters (Φ_{opt}).

[2]This is a modified version of the Farm Error from Equation 4-2, here calculated per wind direction instead of summed across all directions.

The overestimation of wake losses 50° and 120° encountered in Figure 5-6 indicates that the observed overestimation for Turbine 28 in Figure 5-1c and Turbine 15 in Figure 5-2c between 50° and 120° extends to numerous turbines in the wind farm. This overestimation is likely attributed to coastal winds impacting the atmospheric conditions of the incoming wind, resulting in faster wake recovery [69]. While wind speed gradients are considered through heterogeneous inflow modelling, wind rose dependent TI and atmospheric stability are not explicitly accounted for in the models. An investigation of the met mast data analysis in section 3-3 reveals no significant increase in turbulence between 50° and 120°, hinting towards another cause for faster wake recovery. Such a cause could be lower atmospheric stability resulting from coastal winds originating from the corresponding wind directions. However, no data analysis has been conducted on this aspect.

Another notable trend for all optimised models is the zig-zag trend around 139° and 319°. To further examine the wake propagation around these wind directions, the energy ratios of all 36 turbines are analysed for 319° and two bordering wind directions. Figure 5-7 displays the energy ratios of all 36 turbines for wind directions 319°, 304°, and 329° in Figure 5-7a, 5-7b, and 5-7c, respectively. For all three wind directions Turbine 11, 20, 28 and 35 are the upstream turbines for which the SCADA data consistently shows an energy ratio of one, indicating no heterogeneity in the inflow.

First, the energy ratios for a wind direction of 319°, shown in Figure 5-7a, are examined. For this wind direction, the wind farm layout aligns with the incoming wind, and full wake overlap occurs. Each array consists of a significant number of turbines, namely 8 to 12 turbines, with a smaller turbine spacing of 7.2D. The figure demonstrates that, similar to Figure 5-6, the models overestimate wake losses for 319°. While the increased TI from the north (as depicted in Figure 3-2b) contributes to this overestimation, the occurrence of a similar overestimation at 139° (shown in Figure 5-6) suggests that TI is not the only factor. Moreover, as the overestimation is present from the beginning of the arrays, wake superpositioning is unlikely the cause, leaving the exact reason unclear.

An examination of the energy ratios for the bordering wind directions 304° and 329°, in Figure 5-7b and 5-7c respectively, show an overall underestimation of wake losses in wind direction sectors next to the aligned arrays. These wind directions are characterised by partial wake overlap and a larger turbine spacing. Previous validation studies show that engineering wake models tend to overestimate losses in full wake overlap and underestimate losses in partial wake overlap, a phenomenon associated with superposition methods and wake recovery over longer distances. When the error arises farther down in the array, it is often referred to as deep array effects. Comparing the performance of the models in Figure 5-7 and Figure 5-4, it can be observed that most models tend to overestimate wake losses in full wake overlap and underestimate wake losses when partial wake overlap occurs. This is consistent with the findings of, among others, Archer et al. [30] and Hamilton et al. [15]. In the first array in Figure 5-4, all models underestimate wake losses. In the other three arrays, the CC and TurbOPark models show significantly better estimation of the deep array effects. Both models have been proposed as a solution for these deep array effects. Despite the improved performance of these models seen in Figure 5-7b compared to Jensen and GCH, the trend of over- and underestimation persists for Figure 5-7a and 5-7c. Moreover, in Figure 5-7c, it is evident that superpositioning methods may not be the only factor contributing to the divergence, as errors arise at the beginning of the array. To further study this inconsistency, we examine the energy ratio curves of Turbine 4 and 34 in Figure 5-8. For Turbine 34, the

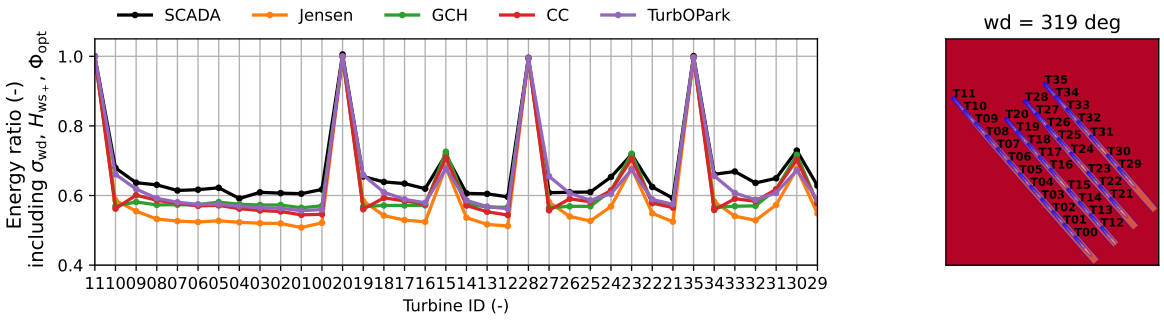

(a) 319°: Wind direction aligns with farm layout, resulting in full wake overlap.

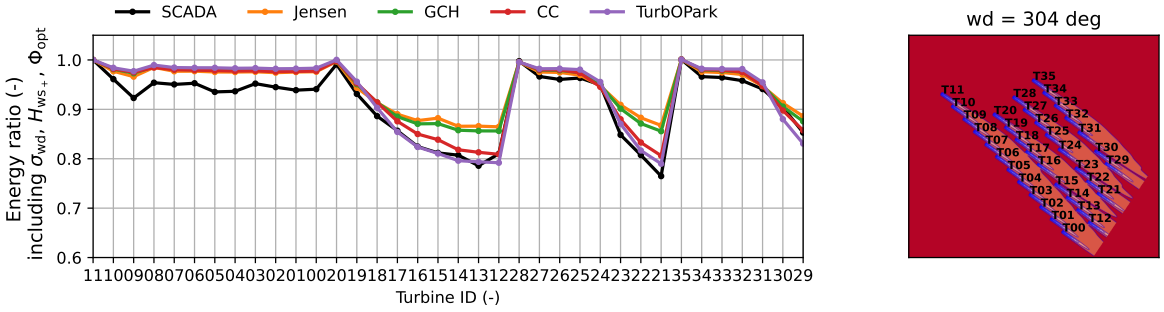

(b) 304°: Wind direction rotated counter-clockwise from 319°, resulting in partial wake overlap.

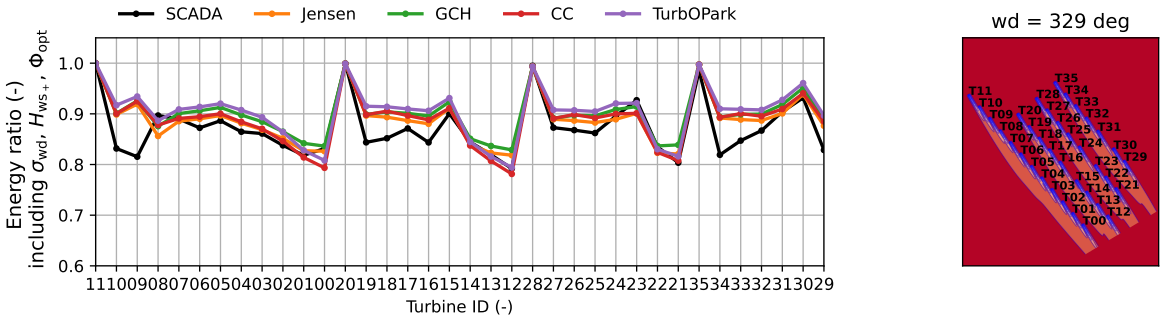

(c) 329°: Wind direction rotated clockwise from 319°, resulting in partial wake overlap.

Figure 5-7: Left: Energy ratios of all 36 turbines for different wind directions after the implementation of wind direction uncertainty (σ_{wd}), heterogeneous inflow wind speeds (H_{ws_+}) and calibrated model parameters (Φ_{opt}). Wind directions include 319° and two neighbouring wind directions 304° and 329°, providing insight into the zig-zag trend observed in Figure 5-6. Right: Flow field visualisation of the OWEZ wind farm for the respective wind directions and wind speed of 8 m/s.

deepest wake loss around 319° in SCADA data and models does not align in the same wind direction, resulting in the underestimation of wake losses in Figure 5-7c. For Turbine 4, where deepest wake loss does both align in 319°, better performance is observed in Figure 5-7c. The investigation of the energy ratio curves for other turbines reveals a similar offset around 319° in Turbines 9, 10, 16, 18, 19, 29, 30, 33, and 34, explaining a part of the underestimation of wake losses observed in Figure 5-7c as well as the overestimation of wake losses in Figure 5-7a. While several inner turbines also show this effect, it is predominantly observed in the outer

turbines of the farm. Additionally, a comparable lack of alignment is found in the energy ratios curves at the deepest wake loss at 139°. This observed shift for both 139° and 319° likely contributes to the zig-zag trends mentioned earlier. The origin of this error is twofold. Firstly, the accuracy and consistency of the SCADA data significantly influence the shape and location of the wake. Note that by including wind direction uncertainty, we only address zero-mean errors, such as measurement noise. Accounting for non-zero-mean errors would require additional steps in the data pre-processing. Secondly, even if the SCADA would be accurate, the models assume a homogeneous wind direction field, with the wind direction equal to the average of all turbines. This assumption may not accurately represent the conditions for all turbines in the farm, particularly those located on the outer edges. For these turbines, spatial variability in the incoming wind direction likely leads to a slight shift compared to the average of all turbines.

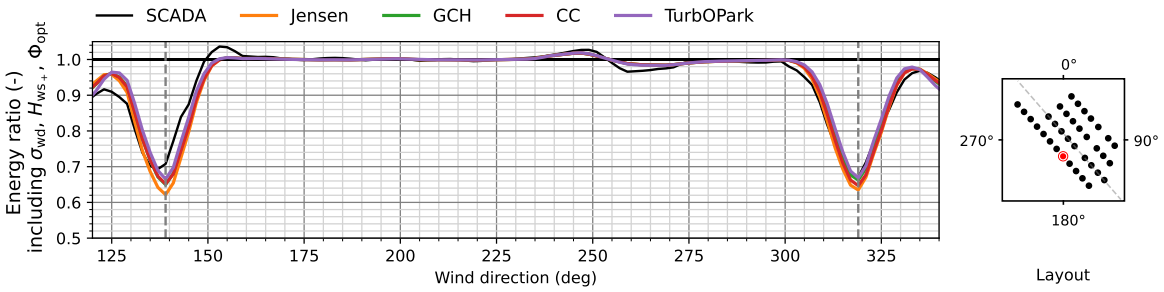

(a) Turbine 4, revealing misalignment of deepest wake loss for 139°.

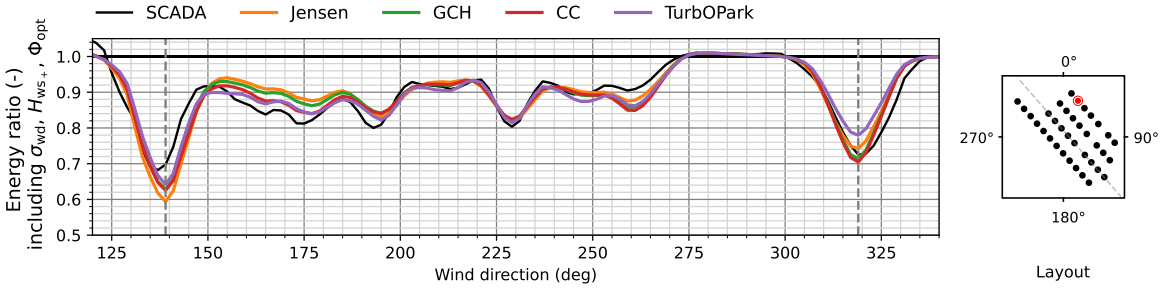

(b) Turbine 34, revealing misalignment of deepest wake loss for 139° and 319°.

Figure 5-8: Left: Energy ratio curves of Turbine 4 and 34 for wind directions between 120° and 340°. Vertical dashed lines mark wind directions aligned with the farm layout (139° and 319°). Right: Layout of the OWEZ wind farm indicating the location of Turbine 4 and 34.

From this subsection, it can be concluded that the proposed validation and calibration framework can significantly increase accuracy across all wind directions. However, discrepancies remain and are likely related to changing atmospheric conditions due to coastal effects and non-zero-mean wind direction uncertainty, which affect all models similarly. Instances of the observed difference in model performance for full and partial wake overlap are likely tied to the fact that these are the wind direction sections where most wake interactions occur. These wind directions also correspond to the regions where model performance diverges. This will be further discussed in the following subsection.

5-3-2 Differences Between Models

The observed variations in model performance are probably linked to the diverse definitions of wake expansion, outlined in chapter 2. Additionally, the CC model employs a novel superpositioning method, whereas the other models use the Sum of Squares method. Analysing where and how model performance diverges provides insights into the efficacy of the different modelling strategies. The comparison of wake models is separated into three scenarios where models deviate most, which will be discussed next.

The first scenario encompasses single wake estimation. It can be observed in Figure 5-3c and Figure 5-7a that TurbOPark consistently predicts lower wake losses at the second turbine in the array than other models. This is accurate for wind directions with a higherTI of 7.8% in Figure 5-7a but not for a TI of 5.3% in Figure 5-3c. Currently, the models do not account for these directional differences and assume a fixed TI of 6.5%. Consequently, it remains unclear which model most accurately estimates single wake loss. If a TI-rose would be implemented in the model input, it can be investigated whether it is affected by how they integrate ambient TI. Moreover, for other wind directions, these distinctions are not evident. Therefore, no clear conclusion can be drawn on this topic.

In the second scenario, involving arrays aligned with the incoming wind direction, as in Figure 5-3c and Figure 5-7a, Jensen performs significantly worse. This is possibly attributable to the fact that Jensen is the only model not including ambient nor turbine-induced TI in its wake expansion.

The third scenario includes situations of partial wake overlap. Both the TurbOPark and CC models have been proposed as a solution for the so-called deep array effects and outperform the Jensen and GCH models in Figure 5-7b. TurbOPark aims to solve the issue by realising a slower wake recovery, and CC by introducing a new superpositioning method. Interestingly, both models achieve similar performance in this scenario by a different method.

Chapter 6

Conclusions and Recommendations

6-1 Conclusions

This master's thesis has introduced a novel framework for the validation and calibration of engineering wake models to answer the research question: *How can the reliability of current engineering wake models be holistically validated for different model applications, and how can reliability be improved by including inflow heterogeneity or parameter calibration?*

The proposed framework combines best practices from literature, accounting for wind direction uncertainty in historical wind farm data and correcting wake model inputs by including heterogeneous inflow wind speeds. Together, these components form the basis for investigating the potential of model parameter calibration to improve the physical characteristics of the wake models. A combination of quantitative and qualitative methods is designed for holistic wake model validation, aiming to reduce the impact of experiment design on perceived model accuracy and enabling comprehensive evaluation of proposed model improvements. The efficacy of this framework was demonstrated through a case study with historical data from the OWEZ wind farm and four engineering wake models from the popular wake modelling tool FLORIS. This has led to the following conclusions.

Firstly, it can be concluded that the designed framework effectively facilitates validation of engineering wake models for different model applications, allows for assessing the effect of validation and calibration steps and can be used to identify, quantify and explain observed variations in model performance. The qualitative and quantitative methods in the framework consist of scenarios and metrics offering insights on farm- and turbine-levels. This approach enables conclusions for varied model applications, such as yield calculations and wake steering. Moreover, the case study has shown that the validation framework holistically evaluated the impact of proposed model improvements, a capability not seen before in the literature. The qualitative analysis illustrated model improvements through energy ratio curves, while the quantitative analysis substantiated these with reduced errors. Additionally, applying this framework to the case study showed that combining the single turbine analysis with an array analysis reveals critical insights. It revealed how the underestimation of wake losses in array analysis might be explained by the

misalignment of the deepest wake losses seen in single turbine analysis. Similarly, the single turbine analysis indicated wind directions with the most significant variations in model performance. Analysing turbine arrays for these wind directions revealed different wake loss propagation patterns among different models. Notably, the CC and TurbOPark models differentiate from the Jensen and GCH models by their improved ability to model deep array effects. These findings confirm the necessity of including both single turbine and turbine array analysis in a wake model validation. This combined approach proposed in the framework reduces the sensitivity to experiment design in current literature and enables deriving generalisable conclusions.

Secondly, it can be concluded that when validating engineering wake models for a specific sector or single wind direction, the impact of wind direction uncertainty in historical data must be considered. This thesis first demonstrated how wind direction uncertainty in SCADA data widens wake profiles compared to those of wake models with a similar total wake loss, affecting validation for specific wind directions. Secondly, it was shown that we can effectively address this uncertainty without losing any information in the SCADA data by including a distribution on the model output. Current validation studies typically overlook this uncertainty, limiting their reliability, or they compensate by widening wind direction bins, which hinders the validation of single wake profiles necessary for wind farm control. It is important to note that this uncertainty does not impact the metric of annual energy production, commonly used in the validation for yield applications, as they aggregate output across all wind directions.

Thirdly, it can be concluded that heterogeneous inflow wind speeds are present in historical data, and the inclusion thereof can improve model accuracy at turbine-level. Firstly, this work has presented a computationally inexpensive method to derive heterogeneous inflow wind speeds from SCADA data. The resulting wind speed gradients revealed patterns indicative of global blockage and background flow likely influenced by coastal effects and the nearby Prinses Amalia Farm. Subsequently, the implementation of heterogeneity revealed a significant impact on turbine performance metrics. The absolute turbine error was reduced up to 20%. This highlights the need to consider wind speed heterogeneity for effective model validation and parameter calibration. Given its effect on turbine accuracy, it is advised to be included when developing wind farm control strategies.

Finally, it can be concluded that calibrating a single wake parameter can significantly improve model accuracy on both farm- and turbine-level, resulting in enhanced performance for most wind directions. Results have demonstrated the potential of parameter calibration to improve the accuracy of engineering wake models, a notable contribution to the field. The calibration of a wake recovery-related parameter to a cost function that minimises turbine error yielded improvements across all validation metrics and was supported by a qualitative analysis. The resulting error reductions reach up to 92% for individual turbines and 65% at farm-level. Given the analysis being limited to one parameter and one wind farm, these findings serve as a starting point for further investigation of calibration potential. Furthermore, after calibration, model performances converge with no significant quantitative differences. Notably, the CC model requires minimal parameter change. In contrast, the TurbOPark model shows the most significant adjustments. Although favoured in the industry for its accuracy in wake loss estimation, these results imply the model is too conservative in its power capture estimates for the OWEZ wind farm. Whether this applies to other wind farms remains uncertain.

6-2 Recommendations

While the findings in this thesis mark significant progress in wake model validation and calibration, they also highlight areas for future research. Recommendations are split into three categories: improving the validation and calibration framework, extending framework applicability to pre-construction scenarios, and implications for industry application.

6-2-1 Framework Development

In the context of framework development, the focus is to expand and improve its capabilities while addressing current limitations.

Firstly, it is recommended to optimise the calibration strategy. This thesis took the first steps in parameter calibration by demonstrating its potential. Future work should focus on refining the calibration process. This includes exploring various cost functions and incorporating uncertainty bounds. Another possibility is calibrating multiple wake model parameters. Before doing so, their correlation must be analysed and potentially mitigated (see, e.g., [35, 41, 68]).

Secondly, it is recommended to focus on improving the reliability of wind direction measurements in historical wind farm data. The non-zero mean errors in wind direction measurements encountered in this thesis currently affect our turbine array analysis. Mitigating these errors will enable a more detailed analysis of differences in model performance for wind directions that are aligned and non-aligned with turbine arrays. To improve the reliability of wind direction measurements, it is suggested to use the average wind direction of three to five turbines neighbouring the analysed turbine instead of taking the average of all turbines. However, this strategy relies on sufficient turbines containing valid wind direction measurements, a condition not met in the OWEZ wind farm data set. Currently, when jumps appear in a turbine's nacelle heading sensor calibration, all its wind direction measurements are classified as faulty, as this hinders the calibration of the measurements to true north. By changing the methodology of the northing calibration and allowing for jumps, the number of turbines whose wind direction measurements are not classified as faulty can be increased. Note that such wind direction errors have minimal impact on the annual energy production validation, which sums over all wind directions. As a result, this modification is not necessary when using the framework for yield validation.

Thirdly, it is recommended to account for wind-direction-dependent atmospheric conditions. Currently, the models assume a fixed turbulence intensity across all wind directions and wind speeds. Comparisons with meteorological mast data reveal that turbulence intensity impacts wake recovery and model accuracy. Additionally, discrepancies due to coastal winds suggest a link to atmospheric stability. This indicates the importance of analysing these factors and developing methods to incorporate them into the framework.

Finally, it is recommended to extend the framework for applicability to turbines in yawed conditions. Future development should include adapting the framework such that it can validate and calibrate wake models under yawed conditions to further assess their suitability for wind farm control.

6-2-2 Pre-Construction Applicability

This thesis demonstrated how parameter calibration and heterogeneous inflow wind speeds impact model accuracy, emphasising their relevance to accurate modelling. As a result, these findings also impact the accuracy of yield calculations and layout optimisation performed during the design of the wind farm. The current framework uses historical data to derive inflow heterogeneity and calibrate parameters. However, such data is unavailable in the pre-construction phase. Therefore, to extend the use of the framework to scenarios lacking historical data, the following recommendations are proposed:

Firstly, it is recommended to test the robustness of calibrated parameters across different offshore wind farms with varying layouts and atmospheric conditions. The case study showed that for the OWEZ wind farm, the CC model required minimal calibration, and the TurbOPark model most. However, these findings do not implicitly apply to all wind farms, as site-specific factors can impact calibration. For example, as highlighted in this thesis, atmospheric stability possibly affects wake recovery and, thereby, the calibration of related parameters. Another site-specific factor, turbine spacing, not covered in this thesis but equally important, is likely to affect calibration as suggested by Van Beek et al. [41]. Consequently, validating the models across offshore wind farms with diverse layouts, sizes, and atmospheric conditions is necessary to further implement the optimised parameters. A model showing minimal sensitivity to site-specific factors during calibration can be an excellent candidate for pre-construction use.

Secondly, it is recommended to develop methods for deriving heterogeneous inflow wind speeds with high-fidelity models. To estimate heterogeneous inflow wind speeds without the availability of SCADA data, we suggest comparing the observed heterogeneity in the historical data with high-fidelity models like Large Eddy Simulations (LES) or mesoscale weather models. LES include both blockage effect and background flow, while mesoscale models can only show background flow. If these models offer similar heterogeneity patterns to the SCADA data, they can be effectively used for pre-construction analysis.

6-2-3 Industry Applications

The proposed framework provides essential insights for both individual turbine- and farm-levels. Hence, it is highly relevant to typical industry applications, including both yield calculations as well as wind farm control and layout optimisation. To further substantiate the conclusions and recommendations made for these applications, we propose the following recommendations:

Firstly, it is recommended to analyse the impact of optimised models on wind farm control and layout optimisation strategies. This thesis has already demonstrated the effect of the framework on yield calculations, primarily driven by parameter calibration. However, further research is needed to evaluate its impact on wind farm control and layout optimisation. Interesting experiments include evaluating whether more accurate models yield greater or lesser power gains when including wind farm control or layout optimisation in a simulation. Alternatively, it would be interesting to investigate which model parameters affect the optimisation outcomes most. Another experiment could include analysing whether more accurate models yield higher gains in wake steering field experiments. The experiments

named above can be used to assess the impact of model improvements and help translate the findings in this thesis into practical application.

Secondly, it is recommended to validate wake models to recently constructed larger-scale wind farms. Most commercial wind farms are rapidly expanding in size, with more and larger turbines. Also, as the number of offshore wind farms placed in close proximity to each other increases, the interactions between neighbouring farms are becoming increasingly important. Therefore, validating with more recently built wind farms is essential for industry relevance. Additionally, the OWEZ case study indicated that both the CC and TurbOPark models outperform the Jensen and GCH models in scenarios with partial wake overlap. While the qualitative performance of CC and TurbOPark is promising, the observed quantitative differences are minimal, potentially due to OWEZ's limited number of turbines and gridded layout. Consequently, further validation in larger-scale wind farms is necessary to confirm the superior accuracy of the CC and TurbOPark models.

6-3 Final Words

In conclusion, this thesis addresses the scientific gaps in the literature by introducing a holistic framework that accounts for previously overlooked factors such as wind direction uncertainty, heterogeneous inflow wind speeds and the sensitivity to experiment design. By doing so, this work sets a new standard in wake model validation. Furthermore, the framework proved the potential of model parameter calibration, paving the way for further model improvement. Ultimately, this thesis contributes to reducing model uncertainty, improving yield estimations, and advancing wake mitigation strategies, collectively increasing the feasibility of wind farms.

Appendix A

Meteorological Mast Analysis

For a comparative analysis of the meteorological mast data and the wind speed and wind direction measurements from the turbines, a subset of the available meteorological mast data recorded during farm operation is used. Only the measurements are included where the meteorological mast is not waked by the OWEZ wind farm, particularly focusing on wind directions between 160° and 300°. To align with the pre-processed SCADA data, the meteorological mast data is filtered to match corresponding time steps. Next, we attempt to identify a consistent time shift by calculating the optimal shift for each month. However, this approach did not yield conclusive results. Consequently, the subsequent analysis proceeds without implementing a time shift.

Figure A-1 presents a comparison of the meteorological mast data with SCADA data from Turbine 3, which retained 74.1% of its data after pre-processing and is not flagged for faulty wind direction measurements during northing calibration. Similar analyses for Turbines 6 and 7 showed comparable outcomes. The first subfigure, Figure A-1a, shows a comparison of wind direction measurements. It reveals a relatively large standard deviation of 13.2° around the mean error of -2.2°. A reason for this large deviation could be the hysteresis of the turbine's yaw angle or misalignment with the incoming wind. The second subfigure, Figure A-1b, depicts a comparison of wind speed measurements. The standard deviation is 0.9 m/s and the mean error is 0.2 m/s. This falls within the uncertainty bounds established in the power curve filtering, which is ± 0.75 m/s.

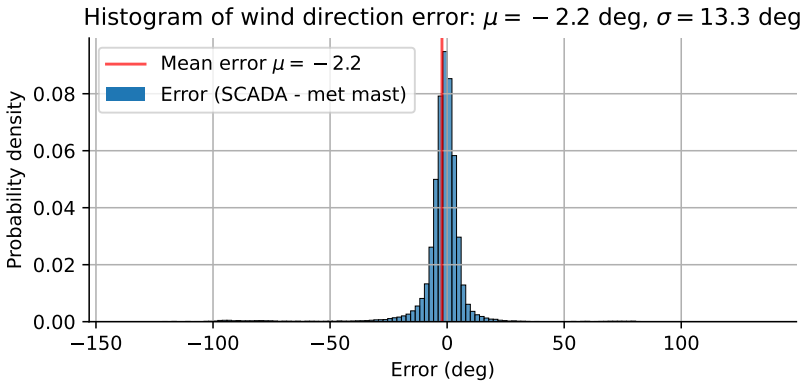

(a) Wind Direction Measurement Comparison: This graph illustrates the comparison between the meteorological mast and turbine wind direction measurements. A mean error of -2.2° and a standard deviation of 13.2° are observed, potentially indicating yaw misalignment or hysteresis effects.

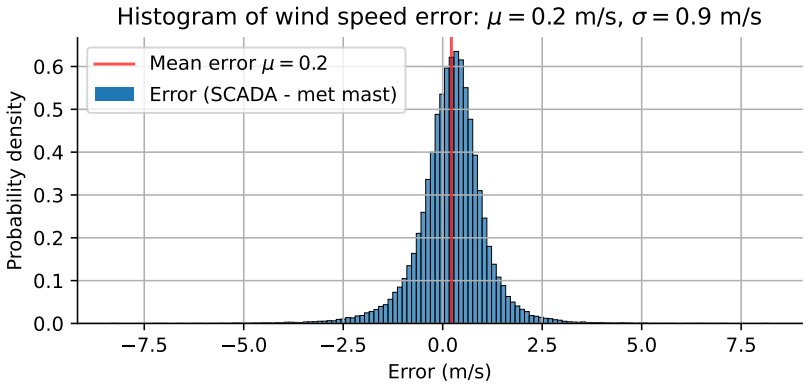

(b) Wind Speed Measurement Comparison: This graph depicts the comparison between the meteorological mast and turbine wind speed measurements. The data shows a mean error of 0.2 m/s with a standard deviation of 0.9 m/s, falling within the established uncertainty bounds of ± 0.75 m/s.

Figure A-1: Comparative analysis of meteorological mast (met mast) and SCADA data of Turbine 3. Data is excluded where the met mast is waked by the wind farm, i.e. wind directions between 160° and 300° are included. This comparison is used to validate turbine sensor accuracy.

Appendix B

Results Inflow Heterogeneity

The results for the various heterogeneous inflow wind speed gradients are displayed in Figure B-1, with each subfigure illustrating the gradient for a particular wind direction. The figure in this section serves two purposes: visualising how such wind speed multiplier is derived for every single turbine and highlighting gradients that are likely caused by common sources of inflow heterogeneity.

First, each single subfigure provides a visualisation of how such a gradient is derived for their specific wind direction. It shows the wind speed multiplier of the upstream turbines. These are obtained by taking the cubic root of the normalised ratios, in accordance with the turbine power-proportional relationship $P_{\text{turbine}} \propto U_{\infty}^{3}$. Moreover, the small dots show how the profile of the upstream turbines is extended downstream along the direction of the incoming wind, advancing the observed gradient across the entire farm. Finally, it provides an overview of the wind speed multipliers of the rest of the turbines.

Second, the subfigures for these wind directions are selected specifically because they show patterns likely attributable to common known causes of inflow heterogeneity. However, it is important to note that these patterns cannot be definitively confirmed. The wind speed gradient in Figure B-1a illustrates a possibility of wind farm blockage, where reduced wind speeds occur at the centre of the farm due to the induction zone of the entire wind farm. Similarly, as shown in Figure B-1b, a speed-up effect is mostly observed on the west edge of the farm. Furthermore, Figure B-1c to B-1f reveal the impact of wakes generated by the Princes Amalia Wind Farm, located [X] kilometres to the west of OWEZ, see Figure 3-1a. These wakes are noticeable for wind directions ranging from 240-270 degrees. Lastly, wind coming from the coast located east of the OWEZ wind farm, see Figure 3-1a, can be recognised by lower wind speeds. This phenomenon could cause lower wind speeds on the east side of the farm for north-east wind direction as shown in Figure B-1g. A similar profile can be observed for south-east wind directions in Figure B-1h.

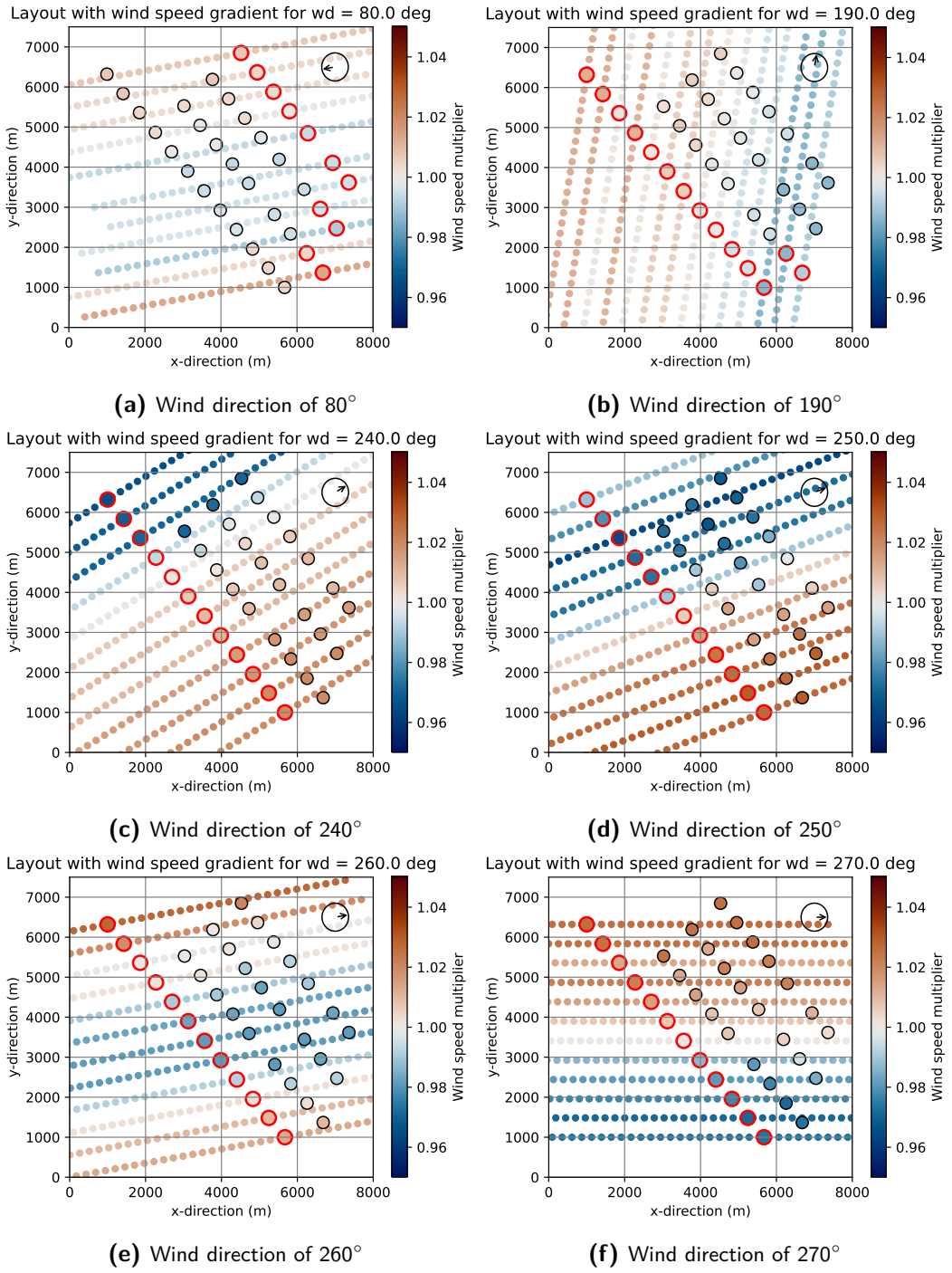

(a) Wind direction of 80°

(b) Wind direction of 190°

(c) Wind direction of 240°

(d) Wind direction of 250°

(e) Wind direction of 260°

(f) Wind direction of 270°

Figure B-1: Wind farm layout showing the derived heterogeneous wind speed gradient for a specific wind direction. The gradient is derived from the cubic root of normalised energy ratios of the red encircled upstream turbines, in accordance with $P_{\text{turbine}} \propto U_{\infty}^{3}$. Small coloured dots indicate the extension of this profile downstream along the direction of the incoming wind, advancing the observed gradient across the entire farm. Black encircled dots represent other turbines with their specific wind speed multipliers. Red indicates higher, and blue indicates lower average incoming wind speeds. The subfigures show patterns likely caused by: **(a)-(b)** Global blockage. **(c)-(f)** Farm-to-farm losses from the neighbouring Prinses Amalia Wind Farm.**(g)-(h)** Lower coastal wind speeds. Note these subfigures continue on the next page.

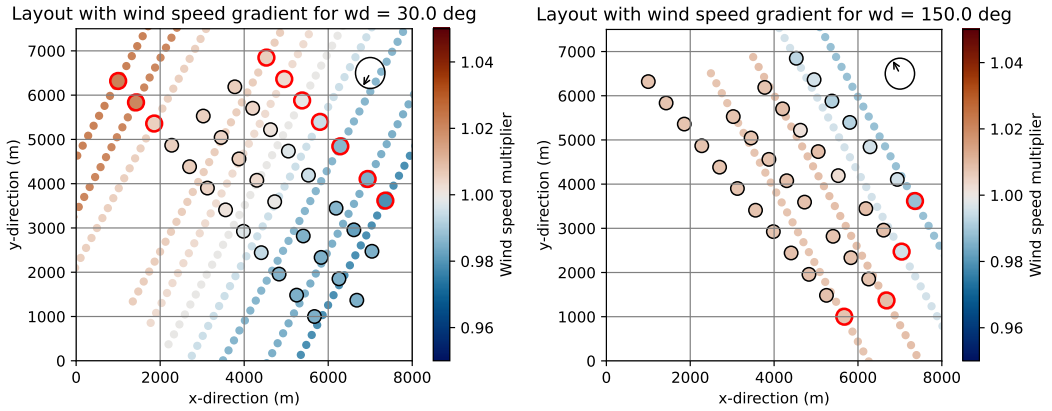

(g) Wind direction of 30°

(h) Wind direction of 150°

Figure B-1: Continued from Figure B-1 on previous page.

Glossary

List of Acronyms

AEP	Annual Energy Production
CC	Cumulative-Curl
FLASC	FLORIS-based Analysis for SCADA data
FLORIS	FLOw Redirection and Induction in Steady State
GCH	Gaussian-Curl-Hybrid
LCOE	Levelised Cost Of Energy
LES	Large Eddy Simulations
NREL	National Renewable Energy Laboratory
NS equations	Navier-Stokes equations
OWEZ	Offshore Windpark Egmond aan Zee
RMSE	Root Mean Square Error
SCADA	Supervisory Control and Data Acquisition
Shell	Shell Global Solutions International B.V.
TI	Turbulence Intensity
TU Delft	Delft University of Technology
TurbOPark	Turbulence Optimised Park
WTG	Wind Turbine Generator

Bibliography

[1] Intergovernmental Panel on Climate Change (IPCC); P.R. Shukla, J. Skea, R. Slade, A. Al Khourdajie, et al. IPPC, 2022: Summary for policymakers. *Climate Change 2022: Mitigation of Climate Change. Contribution of Working Group III to the Sixth Assessment Report of the Intergovernmental Panel on Climate Change*, 2022.

[2] International Energy Agency (IEA). Chart: Renewable power generation by technology in the net zero scenario, 2010-2030. https://www.iea.org/data-and-statistics/charts/renewable-power-generation-by-technology-in-the-net-zero-scenario-2010-2030, Oct 2022. (Accessed on April 6 2023).

[3] International Energy Agency (IEA); S. Bouckaert, A.F. Pales, C. McGlade, U. Remme, B. Wanner, L. Varro, D. D'Ambrosio, and T. Spencer. Net zero by 2050: A roadmap for the global energy sector. *IEA, Paris*, 2021.

[4] A.C. Kheirabadi and R. Nagamune. A quantitative review of wind farm control with the objective of wind farm power maximization. *Journal of Wind Engineering and Industrial Aerodynamics*, 192:45–73, 2019.

[5] E. Gaertner, J. Rinker, L. Sethuraman, F. Zahle, B. Anderson, G.E. Barter, N.J. Abbas, F. Meng, P. Bortolotti, W. Skrzypinski, et al. IEA wind TCP task 37: definition of the IEA 15-megawatt offshore reference wind turbine. Technical report, National Renewable Energy Laboratory (NREL), 2020.

[6] S. Boersma, B.M. Doekemeijer, P.M.O. Gebraad, P.A. Fleming, J. Annoni, A.K. Scholbrock, J.A. F., and J-W. Van Wingerden. A tutorial on control-oriented modeling and control of wind farms. In *2017 American control conference (ACC)*, pages 1–18, 2017.

[7] T. Burton, N. Jenkins, E. Bossanyi, D. Sharpe, and M. Graham. *Wind Energy Handbook*, chapter 2 and 9. John Wiley & Sons, 3rd edition, 2021.

[8] P. Sorensen, T. Nielsen, and M.L. Thogersen. Recalibrating wind turbine wake model parameters—validating the wake model performance for large offshore wind farms. In *European Wind Energy Conference and Exhibition, EWEA*, 2006.

[9] R.J. Barthelmie, S.T. Frandsen, M.N. Nielsen, S.C. Pryor, P-E. Réthoré, and H.E. Jørgensen. Modelling and measurements of power losses and turbulence intensity in wind turbine wakes at middelgrunden offshore wind farm. *Wind Energy*, 10(6):517–528, 2007.

[10] J. Bossuyt, M.F. Howland, C. Meneveau, and J. Meyers. Measurement of unsteady loading and power output variability in a micro wind farm model in a wind tunnel. *Experiments in Fluids*, 58:1–17, 2017.

[11] M.T. van Dijk, J-W. van Wingerden, and Y. Ashuri, T.and Li. Wind farm multi-objective wake redirection for optimizing power production and loads. *Energy*, 121:561–569, 2017.

[12] D.S. Zalkind and L.Y. Pao. The fatigue loading effects of yaw control for wind plants. In *2016 American Control Conference (ACC)*, pages 537–542. IEEE, 2016.

[13] T. Göçmen, P. Van der Laan, P-E. Réthoré, A. Peña, G.C. Larsen, and S. Ott. Wind turbine wake models developed at the technical university of denmark: A review. *Renewable and Sustainable Energy Reviews*, 60:752–769, 2016.

[14] F. Porté-Agel, M. Bastankhah, and S. Shamsoddin. Wind-turbine and wind-farm flows: A review. *Boundary-layer meteorology*, 174:1–59, 2020.

[15] N. Hamilton, C.J. Bay, P.A. Fleming, J. King, and L.A. Martínez-Tossas. Comparison of modular analytical wake models to the lillgrund wind plant. *Journal of Renewable and Sustainable Energy*, 12(5):053311, 2020.

[16] R.J. Barthelmie, K. Hansen, S.T. Frandsen, O. Rathmann, J.G. Schepers, W. Schlez, J. Phillips, K. Rados, A. Zervos, E.S. Politis, et al. Modelling and measuring flow and wind turbine wakes in large wind farms offshore. *Wind Energy: An International Journal for Progress and Applications in Wind Power Conversion Technology*, 12(5):431–444, 2009.

[17] R.J. Barthelmie, S.C. Pryor, S.T Frandsen, K.S. Hansen, J.G. Schepers, K. Rados, W. Schlez, A. Neubert, L.E. Jensen, and S. Neckelmann. Quantifying the impact of wind turbine wakes on power output at offshore wind farms. *Journal of Atmospheric and Oceanic Technology*, 27(8):1302–1317, 2010.

[18] P. Beaucage, M. Brower, N. Robinson, and C. Alonge. Overview of six commercial and research wake models for large offshore wind farms. *Proceedings of the European Wind Energy Associate (EWEA)*, 18, 2012.

[19] M. Gaumond, P-E. Réthoré, A. Bechmann, S. Ott, G.C. Larsen, A. Peña, and K.S. Hansen. Benchmarking of wind turbine wake models in large offshore wind farms. In *Proceedings of the science of making torque from wind conference*, 2012.

[20] M. Gaumond, P-E. Réthoré, A. Ott, A. Peña, A. Bechmann, and K.S. Hansen. Evaluation of the wind direction uncertainty and its impact on wake modeling at the horns rev offshore wind farm. *Wind Energy*, 17(8):1169–1178, 2014.

[21] N.G. Nygaard. Wakes in very large wind farms and the effect of neighbouring wind farms. In *Journal of Physics: Conference Series*, volume 524, page 012162. IOP Publishing, 2014.

[22] N.G. Nygaard. Systematic quantification of wake model uncertainty. In *EWEA Offshore conference*, pages 10–12, 2015.

[23] N.G. Nygaard and A.C. Newcombe. Wake behind an offshore wind farm observed with dual-doppler radars. In *Journal of Physics: Conference Series*, volume 1037, page 072008. IOP Publishing, 2018.

[24] N.G. Nygaard, S. Trads Steen, L Poulsen, and J.G. Pedersen. Modelling cluster wakes and wind farm blockage. In *Journal of Physics: Conference Series*, volume 1618, page 062072. IOP Publishing, 2020.

[25] N.G. Nygaard, L. Poulsen, E. Svensson, and J.G. Pedersen. Large-scale benchmarking of wake models for offshore wind farms. In *Journal of Physics: Conference Series*, volume 2265, page 022008, 2022.

[26] I. Katic, J. Højstrup, and N.O. Jensen. A simple model for cluster efficiency. In *European wind energy association conference and exhibition*, volume 1, pages 407–410, 1986.

[27] C.B. Hasager, P. Vincent, J. Badger, M. Badger, A. Di Bella, A. Peña, R. Husson, and P.J.H. Volker. Using satellite sar to characterize the wind flow around offshore wind farms. *Energies*, 8(6):5413–5439, 2015.

[28] A. Platis, S.K. Siedersleben, J. Bange, A. Lampert, K. Bärfuss, R. Hankers, B. Cañadillas, R. Foreman, J. Schulz-Stellenfleth, B. Djath, et al. First in situ evidence of wakes in the far field behind offshore wind farms. *Scientific reports*, 8(1):2163, 2018.

[29] J. Schneemann, A. Rott, M. Dörenkämper, G. Steinfeld, and M. Kühn. Cluster wakes impact on a far-distant offshore wind farm's power. *Wind Energy Science*, 5(1):29–49, 2020.

[30] C.L. Archer, A. Vasel-Be-Hagh, C. Yan, S. Wu, Y. Pan, J.F. Brodie, and A.E. Maguire. Review and evaluation of wake loss models for wind energy applications. *Applied Energy*, 226:1187–1207, 2018.

[31] B.M. Doekemeijer, E. Simley, and P.A. Fleming. Comparison of the gaussian wind farm model with historical data of three offshore wind farms. *Energies*, 15(6):1964, 2022.

[32] M. Bastankhah and F. Porté-Agel. Experimental and theoretical study of wind turbine wakes in yawed conditions. *Journal of Fluid Mechanics*, 806:506–541, 2016.

[33] C.J. Bay, P.A. Fleming, B.M. Doekemeijer, J. King, M. Churchfield, and R. Mudafort. Addressing deep array effects and impacts to wake steering with the cumulative-curl wake model. *Wind Energy Science*, 8(3):401–419, 2023.

[34] M. Bastankhah, B.L. Welch, L.A. Martínez-Tossas, J. King, and P.A. Fleming. Analytical solution for the cumulative wake of wind turbines in wind farms. *Journal of Fluid Mechanics*, 911:A53, 2021.

[35] J. Schreiber, C.L. Bottasso, B. Salbert, and F. Campagnolo. Improving wind farm flow models by learning from operational data. *Wind Energy Science*, 5(2):647–673, 2020.

[36] F. Campagnolo, L. Imširović, R. Braunbehrens, and C.L. Bottasso. Further calibration and validation of floris with wind tunnel data. In *Journal of Physics: Conference Series*, volume 2265, page 022019, 2022.

[37] P.M.O. Gebraad, F.W. Teeuwisse, J-W. Van Wingerden, P.A. Fleming, S.D. Ruben, J.R. Marden, and L.Y. Pao. Wind plant power optimization through yaw control using a parametric model for wake effects—a cfd simulation study. *Wind Energy*, 19(1):95–114, 2016.

[38] P.A. Fleming, J. Annoni, J.J. Shah, L. Wang, S. Ananthan, Z. Zhang, K. Hutchings, P. Wang, W. Chen, and L. Chen. Field test of wake steering at an offshore wind farm. *Wind Energy Science*, 2(1):229–239, 2017.

[39] B.M. Doekemeijer, J-W. Van Wingerden, and P.A. Fleming. A tutorial on the synthesis and validation of a closed-loop wind farm controller using a steady-state surrogate model. In *2019 American Control Conference (ACC)*, pages 2825–2836. IEEE, 2019.

[40] M.F. Howland, S.K. Lele, and J.O. Dabiri. Wind farm power optimization through wake steering. *Proceedings of the National Academy of Sciences*, 116(29):14495–14500, 2019.

[41] M.T. van Beek, A. Viré, and S.J. Andersen. Sensitivity and uncertainty of the floris model applied on the lillgrund wind farm. *Energies*, 14(5):1293, 2021.

[42] A. Farrell, J. King, C. Draxl, F. Mudafort, N. Hamilton, C.J. Bay, P. Fleming, and E. Simley. Design and analysis of a wake model for spatially heterogeneous flow. *Wind Energy Science*, 6(3):737–758, 2021.

[43] P.A. Fleming, J. King, K. Dykes, E. Simley, J. Roadman, A. Scholbrock, P. Murphy, J.K. Lundquist, P. Moriarty, K. Fleming, et al. Initial results from a field campaign of wake steering applied at a commercial wind farm–part 1. *Wind Energy Science*, 4(2):273–285, 2019.

[44] P.A. Fleming, J. King, E. Simley, J. Roadman, A. Scholbrock, P. Murphy, J.K> Lundquist, P. Moriarty, K. Fleming, J. van Dam, et al. Continued results from a field campaign of wake steering applied at a commercial wind farm–part 2. *Wind Energy Science*, 5(3):945–958, 2020.

[45] P.A. Fleming, M. Sinner, T. Young, M. Lannic, J. King, E. Simley, and B.M. Doekemeijer. Experimental results of wake steering using fixed angles. *Wind Energy Science*, 6(6):1521–1531, 2021.

[46] E. Simley, P. Fleming, N. Girard, L. Alloin, E. Godefroy, and T. Duc. Results from a wake-steering experiment at a commercial wind plant: investigating the wind speed dependence of wake-steering performance. *Wind Energy Science*, 6(6):1427–1453, 2021.

[47] N.F. Baker, A.P. Stanley, J.J. Thomas, A. Ning, and K. Dykes. Best practices for wake model and optimization algorithm selection in wind farm layout optimization. In *AIAA Scitech 2019 forum*, page 0540, 2019.

[48] Puyi Yang and Hamidreza Najafi. The effect of using different wake models on wind farm layout optimization: A comparative study. *Journal of Energy Resources Technology*, 144(7):070904, 2022.

[49] NREL. FLORIS. version 3.3. https://github.com/NREL/floris, March 2023. (Accessed on April 24 2023).

[50] M.J. van den Broek, M. Becker, B. Sanderse, and J-W. van Wingerden. Dynamic wind farm flow control using free-vortex wake models. *Wind Energy Science Discussions*, 2023:1–28, 2023.

[51] M.M. Pedersen, van der Laan P. Forsting, A.M., R. Riva, L.A.A. Romàn, J.C. Risco, M. Friis-Møller, J. Quick, J.P.S. Christiansen, R.V. Rodrigues, B.T. Olsen, and P-E. Réthoré. Pywake 2.5.0: An open-source wind farm simulation tool. 2 2023.

[52] N.O. Jensen. *A note on wind generator interaction*, volume 2411. Citeseer, 1983.

[53] J. Schmidt and L. Vollmer. Industrial wake models. In *Handbook of Wind Energy Aerodynamics*, pages 1–28. Springer, 2021.

[54] L.P. Chamorro and F. Porté-Agel. A wind-tunnel investigation of wind-turbine wakes: boundary-layer turbulence effects. *Boundary-layer meteorology*, 132:129–149, 2009.

[55] Y-T. Wu and F. Porté-Agel. Atmospheric turbulence effects on wind-turbine wakes: An les study. *energies*, 5(12):5340–5362, 2012.

[56] S. Xie and C. Archer. Self-similarity and turbulence characteristics of wind turbine wakes via large-eddy simulation. *Wind Energy*, 18(10):1815–1838, 2015.

[57] A. Crespo, J. Herna, et al. Turbulence characteristics in wind-turbine wakes. *Journal of wind engineering and industrial aerodynamics*, 61(1):71–85, 1996.

[58] M. Bastankhah and F. Porté-Agel. A new analytical model for wind-turbine wakes. *Renewable energy*, 70:116–123, 2014.

[59] A. Niayifar and F. Porté-Agel. Analytical modeling of wind farms: A new approach for power prediction. *Energies*, 9(9):741, 2016.

[60] L.A. Martínez-Tossas, J. Annoni, P.A. Fleming, and M.J. Churchfield. The aerodynamics of the curled wake: a simplified model in view of flow control. *Wind Energy Science*, 4(1):127–138, 2019.

[61] J. King, P.A. Fleming, R. King, L.A. Martínez-Tossas, C.J. Bay, R. Mudafort, and E. Simley. Control-oriented model for secondary effects of wake steering. *Wind Energy Science*, 6(3):701–714, 2021.

[62] P.B.S. Lissaman. Energy effectiveness of arbitrary arrays of wind turbines. *Journal of Energy*, 3(6):323–328, 1979.

[63] F. Blondel and M. Cathelain. An alternative form of the super-gaussian wind turbine wake model. *Wind Energy Science*, 5(3):1225–1236, 2020.

[64] J.G. Pedersen, E. Svensson, L. Poulsen, and N.G. Nygaard. Turbulence optimized park model with gaussian wake profile. In *Journal of Physics: Conference Series*, volume 2265, page 022063, 2022.

[65] S. Frandsen, R. Barthelmie, S. Pryor, O. Rathmann, S. Larsen, J. Højstrup, and M. Thøgersen. Analytical modelling of wind speed deficit in large offshore wind farms. *Wind Energy*, 9(1-2):39–53, 2006.

[66] NREL. FLASC. version 1.2. https://github.com/NREL/flasc, November 2022. (Accessed on April 24 2023).

[67] L. Kemme, S. Strnad, L. Vollmer, J. Schmidt, and L.J. Lukassen. Sensitivity of wake modelling setups. In *Journal of Physics: Conference Series*, volume 2265, page 022007, 2022.

[68] D. van Binsbergen, P-J. Daems, T. Verstraeten, A. Nejad, and J. Helsen. Hyperparameter tuning framework for calibrating analytical wake models using scada data of an offshore wind farm applied on floris. *Wind Energy Science Discussions*, 2023:1–28, 2023.

[69] R.J. Barthelmie, M.J. Churchfield, P.J. Moriarty, J.K. Lundquist, G.S. Oxley, S. Hahn, and S.C. Pryor. The role of atmospheric stability/turbulence on wakes at the egmond aan zee offshore wind farm. In *Journal of Physics: Conference Series*, volume 625, page 012002. IOP Publishing, 2015.